Title

Extensive, transient, and long-lasting gene regulation in a song-controlling brain area during testosterone-induced song development in adult female canaries

Authors

Meng-Ching Ko[1*], Carolina Frankl-Vilches[1], Antje Bakker[1], Nina Sohnius-Wilhelmi[1], Manfred Gahr[1]

Affiliations

[1] Department of Behavioural Neurobiology, Max Planck Institute for Biological Intelligence (in foundation; ex-Max Planck Institute for Ornithology), Seewiesen, 82319, Germany. * Corresponding author, E-mail: mcko@orn.mpg.de

Abstract

Like other canary reproductive behaviors, song production occurs seasonally and can be triggered by gonadal hormones. Adult female canaries treated with testosterone sing first songs after four days and progressively develop towards typical canary song structure over several weeks, a behavior that females otherwise rarely or never show. We compared gene regulatory networks in the song-controlling brain area HVC after 1 hour (h), 3 h, 8 h, 3 days (d), 7d, and 14d testosterone treatment with placebo-treated control females, paralleling HVC and song development. Rapid onset (1 h or less) of extensive transcriptional changes (2,700 genes) preceded the onset of song production by four days. The highest level of differential gene expression occurred at 14 days when song structure was most elaborate, and song activity was highest. The transcriptomes changed massively several times during the two-week of song production. A total of 9,710 genes were differentially expressed, corresponding to about 60% of the known protein-coding genes of the canary genome. Most (99%) of the differentially expressed genes were regulated only at specific stages. The differentially expressed genes were associated with diverse biological functions, of which cellular level occurring early and nervous system level occurring primarily after prolonged testosterone treatment. Thus, the

development of adult songs requires restructuring the entire HVC, including most HVC cell types, rather than altering only neuronal subpopulations or cellular components. Parallel regulation directly by androgen and estrogen receptors and by other hub genes such as the transcription factor SP8, which are under steroidogenic control, lead to massive transcriptomic and neural changes in the specific behavior-controlling brain areas and gradual seasonal occurrence of singing behavior.

Introduction

Adult socio-sexual behaviors of vertebrates emerge seasonally or otherwise transiently in most vertebrate species. They are under the control of gonadal hormones (androgens and estrogens), which increase and decrease due to phasic neuroendocrine regulation of the gonadal activity triggered by environmental conditions (Ball and Balthazart, 2002; Guh et al., 2019; Weems et al., 2015). In addition, seasonal changes in brain areas' sensitivities for gonadal hormones are important for the seasonal occurrence of reproductive behaviors (Quispe et al., 2015; Riters et al., 2000; Schlinger et al., 1984; Sharp et al., 1986; Watts, 2020). This seasonality of behaviors and underlying sensory and motoric brain functions seems to be due to gonadal hormone-dependent activation of existing neural circuits of adult individuals, and, in some cases, changed configuration of neural circuits (Celec et al., 2015; Forlano et al., 2015; Jennings and de Lecea, 2020; Migaud et al., 2015; Schwartz and Andrews, 2013; Zornik and Kelley, 2011). A prominent latter example is the seasonal singing of some songbird species, which coincides with a seasonal change of morphology of song controlling brain regions (Alliende et al., 2017; Apfelbeck et al., 2012; Ball et al., 2004; de Bournonville et al., 2021; Gahr, 2004; Gahr, 2020; Nottebohm, 1981). However, even in such examples, not all cell populations behave seasonal, hence the neuronal seasonal plasticity seems to be limited to certain cells (Gahr, 1990b; Gahr and Metzdorf, 1997; Leitner et al., 2001).

Binding of androgens and estrogens to their respective receptors (the androgen receptor (AR), the estrogen receptor α/ß (ESR1/2)) triggers transcription of a gene cascade or exerts non-genomic

52 actions by activating intracellular second messenger pathways (Celec et al., 2015; Fuentes and Silveyra,
53 2019). During differentiation processes, the androgen and estrogens seem to activate a few tissue-
54 specific hub-genes, and subsequently initiate tissue-specific cascades, which regulate several tens or
55 hundreds of genes in a given tissue and determine the tissue's function (Pihlajamaa et al., 2015). In
56 adults, while the gonadal hormones might affect several regions of a neural circuit, the affected gene
57 cascades of a particular brain region seem limited (Bao et al., 2019; Peterson et al., 2013; Schwartz et
58 al., 2013; Zhang et al., 2016; Zhao et al., 2021). However, it is particularly unclear what such gonadal
59 hormone-triggered cascades might be if the induced behavior emerges slowly over many days to weeks,
60 which is typical for seasonal behaviors such as the singing of canaries (Nottebohm et al., 1986; Voigt
61 and Leitner, 2008). The dynamic interplay between hormones, gene expression, brain structure, and
62 behavior is challenging to study.

63 Singing behavior is a complex behavior that involves intensive integration of sensory inputs
64 and motor outputs (Wild, 2004). Songbirds use their songs in various reproductive contexts, including
65 mate attraction (Byers et al., 2010; Drăgănoiu et al., 2002), pair bond formation (Wickler and Seibt,
66 1980), and territorial defense (Catchpole and Slater, 2018; Snijders et al., 2017). In many North
67 temperate species, this sexually motivated singing behavior concerns only the males and is sensitive
68 to testosterone and its androgenic and estrogenic metabolites (Gahr, 2014). In some species, females
69 can sing in a sexual context however females sing frequently in a non-breeding context (Gahr, 2020;
70 Riebel et al., 2019). Nevertheless, in adult males and females of most bird species, including those in
71 which the function of female singing is unclear, testosterone treatment increased the singing rates
72 and/or changed the species-specific song pattern (Dittrich et al., 2014; Gahr, 2020; Hausberger et al.,
73 1995).

74 The neural song control system of songbirds (Nottebohm et al., 1976; Wild, 2004) is a target
75 of testosterone due to the abundant expression of androgen and estrogen receptors (Gahr, 1990b;
76 Johnson and Bottjer, 1995; Metzdorf et al., 1999). The premotor forebrain nucleus HVC is a

77 sensorimotor integration center of the song system (Hahnloser et al., 2002; Yu and Margoliash, 1996)
78 that controls the temporal pattern of singing (Hahnloser et al., 2002; Long and Fee, 2008). It is the
79 only song control nucleus that expresses both androgen and estrogen receptors (Frankl-Vilches and
80 Gahr, 2017; Gahr, 2001), suggesting extensive hormonal regulation of various organizational levels of
81 the HVC. For example, previous studies have shown that angiogenesis occurs in the HVC of adult
82 female canaries within one week of testosterone treatment and is mediated by a testosterone metabolite,
83 17β-estradiol (Louissaint et al., 2002), testosterone induces gap junctions in the HVC (Gahr and
84 Garcia-Segura, 1996) and androgens induce the pruning of spines of HVC neurons (Vellema et al.,
85 2019). A handful of studies documented the endpoint of transcriptomic changes in songbird brains in
86 response to several weeks of testosterone treatment (Dittrich et al., 2014; Frankl-Vilches et al., 2015;
87 Larson et al., 2015; Peterson et al., 2013; Thompson et al., 2012). However, the transcriptomic effects
88 at the onset of testosterone-driven singing and the progression of gene expression cascades associated
89 with anatomical changes in the song control system and the development of singing behavior are not
90 studied

91 Female canaries (*Serinus canaria*) rarely sing (Hartley et al., 1997; Herrick and Harris, 1957;
92 Ko et al., 2020; Pesch and Güttinger, 1985), and the complexity of spontaneous female canary songs
93 is different from that of male songs (Ko et al., 2020). However, non-singing female canaries begin to
94 sing simple songs after testosterone treatment, and the song structure improves during the weeks of
95 testosterone treatment (Hartog et al., 2009; Ko et al., 2020; Shoemaker, 1939; Vallet et al., 1996;
96 Vellema et al., 2019), similar to the seasonal emergence of singing in male birds. The administration
97 of testosterone induces differentiation of brain nuclei involved in song control in adult female canaries,
98 which is considered crucial for song development (Fusani et al., 2003; Madison et al., 2015;
99 Nottebohm, 1980). Thus, testosterone-treated female canaries are an excellent model to monitor the
100 transcriptional cascades in parallel with differentiation of the song control system and the progressing
101 song development.

102 Here, we examine the short- and long-term responses of HVC gene expression after
103 testosterone treatment. We implanted adult female canaries with testosterone over six time periods (1
104 hour (h) [T1h], 3 h [T3h], 8 h [T8h], 3 days (d) [T3d], 7 d [T7d], and 14 d [T14d]; Fig. 1A-B and Table
105 1) and monitored their vocal activity. We quantified gene expression and linked the transcriptomic
106 data to neuroanatomical and behavioral measurements of the implanted birds to identify the key
107 molecular players in testosterone-driven song development. In contrast to our expectation that
108 testosterone regulates only a small number of genes at the beginning of implantation and then gradually
109 recruits more and more genes, our results show that testosterone rapidly alters adult HVC gene
110 expression in a very strong and gene-dependent, dynamic, or constant manner. After an initial fast
111 change in transcription (1 hour) which concerned already 2,652 genes, the differential gene expression
112 changes dynamically and is boosted after about 14 days of testosterone treatment altering the
113 expression of 7,702 genes including 730 transcription factors. Our study demonstrates the progression
114 of cellular and network-level events in the HVC that seem required for the initiation and development
115 of singing behavior.
116

117 **Results**

118 We selected non-singing females to obtain a homogenous baseline for testosterone-induced song
119 development in all experimental animals and observed song activity after hormone implantation to
120 determine the timing of testosterone-induced song development (Fig. 1). After testosterone
121 implantation, birds in groups T1h, T3h, T8h, and T3d either called or were silent and did not sing
122 whereas five of six birds in group T7d and all birds in group T14d sang (Supplementary Fig. 1 and
123 Supplementary Table 1). On average, the first recognizable subsongs were uttered 4.1 ± 1.6 (mean ±
124 SD) days after implantation, similar to previous reports (Vellema et al., 2019) and similar to the time
125 required for male canaries to sing in the nonbreeding season when implanted with testosterone (Sartor

126 et al., 2005). One female of the T14 group sang already one day after testosterone treatment. Singing
127 activity increased significantly after day 2 and day 10 of testosterone treatment; there was no statistical
128 difference in singing activity between day 2 to day 9 (Fig. 1C, Supplementary Table 2, and
129 Supplementary Table 3).
130

131 **Testosterone-induced progressive song development.**

132 At the onset of song development, the songs showed a large inter- and intra-individual variability
133 (Supplementary Fig. **2** and Supplementary Table 1). Testosterone significantly increased the song
134 lengths daily until day 7, and further increased the song lengths from day 11 (Fig. 1D, Supplementary
135 Table 2, and Supplementary Table 3). Similarly, the number of syllables per song also increased daily
136 after implantation (Fig. 1E). Testosterone implantation significantly increased syllable repetition rate
137 in two steps, first on day 2 and then on day 9 (Fig. 1F). The maximum syllable repetition rate of all
138 songs was 26 Hz, which is consistent with a previous study (Fusani et al., 2003).
139

140 **Testosterone increased HVC volume after two weeks.**

141 HVC volumes were significantly greater in T14d birds than in controls (Fig. 1G, CON: 0.103 ± 0.039
142 mm^3 (mean ± SD); T14d: 0.253 ± 0.087 mm3, Kruskal-Wallis followed by Dunn post hoc test, χ^2 =
143 16.55, df = 6, Holm-adjusted P-value = 0.020). The HVC volumes of T7d were not significantly
144 different from those of controls (T7d: 0.146 ± 0.073 mm3, Holm-adjusted P-value = 1.00) and were
145 not different from those of T14d because of the wide variation in HVC volumes of T7d (Holm-adjusted
146 P-value = 0.732). Testosterone-treated birds were not significantly different from controls in terms of
147 brain weight, body weight, and oviduct weight (Supplementary Fig. 4A-C). HVC volumes normalized
148 with respect to brain weight yielded the same results as those without normalization (Kruskal-Wallis
149 followed by Dunn post hoc test, χ^2 = 17.86, df = 6, Supplementary Fig. 4D). The HVC development
150 observed is consistent with previous findings that systemic administration of testosterone results in

151 detectable HVCs in female canaries (Cornez et al., 2020; Fusani et al., 2003; Hartog et al., 2009;
152 Madison et al., 2015; Nottebohm, 1980; Rasika et al., 1994).
153

154 **Testosterone dramatically altered transcriptomes of the HVC.**

155 To investigate the effect of testosterone on gene regulation of the HVC, we performed microarray
156 analyses and examined the different gene expression profiles of the six testosterone-treated groups
157 compared with controls. We used microarrays for the transcriptome analysis to cope with the small
158 amounts of mRNA that is available from the HVCs of an individual female. The effect of testosterone
159 on transcription was evident as early as 1 hour after implantation (T1h, Fig. 3A), when plasma
160 androgen levels were significantly elevated (Fig. 1B; see Methods). The expression levels of 2,652
161 genes were significantly different between T1h and controls; 1,539 genes were upregulated and 1,113
162 were downregulated, including 141 up-regulated transcription factors (TFs) and 80 down-regulated
163 TFs (Fig. 3A). The number of differentially expressed genes fluctuated during testosterone treatment
164 and increased dramatically after 14 days (T14d, Fig. 3A). At 14 days, 5,632 genes were upregulated
165 and 2,070 downregulated, including 525 upregulated and 205 downregulated TFs. These 7,702 genes
166 represent 49% of all currently known protein-coding genes of the canary genome (Frankl-Vilches et
167 al., 2015). Overall, testosterone treatment affected the expression of 9,710 genes across all time points
168 combined, corresponding to approximately 60% of all canary protein-coding genes (Frankl-Vilches et
169 al., 2015).
170

171 **The vast majority of testosterone-induced genes were only transiently affected.**

172 To gain insight into the temporal dynamics of gene expression altered by testosterone, we classified
173 the differentially expressed genes into four classes: 1) constantly upregulated (at all six time points),
174 2) constantly downregulated, 3) dynamically regulated genes that the direction of regulation varied
175 between time points, and 4) transiently regulated genes whose expression was altered at least at one

176 but not all time points (Fig. 3B). In contrast to our expectation that testosterone regulates a small
177 number of genes at the beginning of implantation and gradually recruits more and more genes, we
178 observed a rapid and massive effect in a nonlinear dynamic regulatory style. The majority of genes
179 differentially expressed after testosterone treatment were transiently regulated genes (9,557 genes). In
180 contrast, the abundance of genes in the constant-regulated classes was much lower, with approximately
181 50 genes in each class (Fig. 3B). Constantly upregulated genes included pluripotent genes such as the
182 transcription factors *FLII* (FLII actin remodeling protein) and *NOTCH1* (notch receptor 1), which are
183 associated with a variety of cellular processes such as morphogenesis of anatomical structures
184 (Limbourg et al., 2005) (Supplementary Table 4). Constantly downregulated genes included genes
185 associated with apoptosis, such as *CASP8AP2* (caspase 8-associated protein 2) and *MAPK14* (mitogen-
186 activated protein kinase 14) (Jia et al., 2009) (Supplementary Table 4).

187 **Parallel direct and indirect regulation of many genes by nuclear steroid receptors.**

188 To evaluate the possibility of widespread parallel regulation of the expression of the many
189 testosterone-influenced genes by the nuclear gonadal steroid receptors (AR, ESR1, and ESR2), we
190 screened the promoter sequences of the upregulated genes for androgen and estrogen response
191 elements (AREs and EREs, respectively) using the Genomatix-overrepresented TFBS tool. If many
192 promoter sequences of testosterone-regulated genes contained AREs or EREs, nuclear steroid
193 receptors could directly regulate such genes in parallel and rapidly cause extensive changes in the HVC
194 transcriptome. Indeed, both AREs (V$ARE.04) and EREs (V$ER.02, V$ER.03, V$ER.04, and
195 V$ESR2.01) were overrepresented in the promoter sequences of genes that were upregulated within 1
196 hour of testosterone treatment (Supplementary Table 5), which concerned 83.7 % of 962 differentially
197 expressed genes with available promoter sequences. AREs were identified in 45.9% (442), ERE in
198 7.4% (71) and both ARE and ERE in 30.4% (292) of the promoter sequences of differentially expressed
199 genes. In addition, approximately 9% of the genes upregulated in T1h are transcription factors (141
200 genes, Fig. 3A); the MatInspector tool of the Genomatix software suite identified AREs and/or EREs

201 in the 31 promoters of the 38 transcription factors whose promoter sequences we were able to obtain
202 (see Supplementary Table 6).

203 After 14 days, when differential gene expression increased massively, the number of
204 differentially transcribed transcription factors was much higher in T14d transcriptomes compared to
205 all other time points (Fig. 3A). Overall, however, the frequency of genes with ARE (48.2%), ERE
206 (7.6%), or both (26.3%) (total 82.1%) among 2941 promoter-sequence-available differentially
207 expressed genes in T14d-HVCs was similar to that in T1d-HVCs. Therefore, testosterone-controlled
208 hub genes such as transcription factor SP8 (see below), in addition to androgen and estrogen receptors,
209 may have caused strongly increased transcriptional regulation in the HVC at 14 days of song
210 development.

211 **Testosterone affected steroid homeostasis and steroid receptor expression in the HVC.**

212 Testosterone can be converted by aromatase (CYP19A1) to the major estrogen 17β-estradiol, by 5α-
213 reductase (SRD5A2) to the active androgen 5α-dihydrotestosterone (5α-DHT), or by 5β-reductase
214 (AKR1D1) to the inactive androgen 5β-dihydrotestosterone (5β-DHT) (Michels and Hoppe, 2008).
215 The active forms of androgens and estrogens can trigger transcription via nuclear androgen and
216 estrogen receptors.

217 One hour after implantation, the HVC cells appear to act to lower local testosterone and
218 estradiol levels. For example, *AKR1D*1 was upregulated, possibly reducing active androgen levels by
219 promoting the conversion of testosterone to inactive 5β-DHT (Fig. 2E). In addition, upregulation of
220 UDP-glucuronosyltransferase 1A (*UGT1A1* and *UGT1A9*) could reduce the toxicity of 17β-estradiol
221 through conjugation of hydrophilic glucuronides (Guillemette, 2003; Ouzzine et al., 2014). In contrast,
222 the HVC appears to have adjusted to elevated testosterone levels eight hours after implantation:
223 *AKR1D1* and *UGT1A1* were downregulated again, and *SRD5A2* was upregulated instead (Fig. 2C, 2D,
224 and 2E). In addition, *ESR1* (estrogen receptor α) was now upregulated.

225 After two weeks of treatment, many genes encoding enzymes involved in steroidogenesis and
226 steroid activity were up-regulated, including *HSD3B2*, *CYP17A1*, *SRD5A2*, *CYP19A1*, *ARK1D1*
227 (except for the down-regulation of *HSD17B12*), the nuclear steroid receptors (*AR* and *ESR2*) as well
228 as the membrane-associated androgen receptor *GPRC6A* (Pi et al., 2010) (Fig. 2E). The up-regulation
229 of many steroidogenesis enzymes and receptors suggests potentially active biosynthesis of various
230 steroidogenesis metabolites capable of triggering hormone signaling cascades. This might contribute
231 to the high number of differentially expressed genes at T14d.

232 **Testosterone-induced genes were first associated with cellular changes and at later**
233 **stages associated with neural system changes.**

234 We performed Gene Ontology (GO) term enrichment analysis to predict potential biological processes
235 of the HVC affected by testosterone implantation at different time points (Fig. 3C and Supplementary
236 Table 7). After one hour of testosterone treatment, genes associated with processes such as circulatory
237 system development (GO:0072359), cell development (GO:0048468), and neuron development
238 (GO:0048666) were enriched, and genes associated with neurogenesis (GO:0022008) were enriched
239 after three hours. Many processes associated with cellular anatomical changes showed continuous
240 enrichment from T1h to T14d. We refined the above enrichment analyses with the foci on HVC cell
241 types, neuronal protrusions, and neuronal activities. In cell type analysis, we observed enrichment for
242 genes associated with "oligodendrocytes" and "endothelial cells" at two specific time points (T3h and
243 T7d, Fig. 3D, Supplementary Table 8 and Supplementary Table 9). In contrast, genes associated with
244 "projection neurons" were enriched at almost all time points examined, with both upregulated and
245 downregulated genes. Genes associated with "interneurons" and "microglia" were not enriched in the
246 testosterone-regulated ones. However, since testosterone changed the transcription of genes involved
247 in GABA signaling (see below), interneurons, too, were affected. For testosterone-sensitive genes
248 related to neuronal morphology, we found that genes associated with "axon," "myelin," "dendrites,"
249 and "spine" were enriched as early as one hour after testosterone treatment and at all later time points

250 examined. We further investigated whether testosterone regulates electrical or chemical synapses and
251 thus influences neuronal activities by evaluating additional search terms, including gap junction, eight
252 different neurotransmitters, their receptors, and genes involved in the biosynthesis of those
253 neurotransmitters (Fig. 3). We found no enrichment of "gap junction" in the time window of our
254 experiment. Among the eight neurotransmitters examined, only the genes associated with "glutamate"
255 and "GABA" showed enrichment. Genes downregulated by testosterone were enriched for glutamate
256 at T3h, T8h, and T14d (Supplementary Table 9). The genes associated with the inhibitory
257 neurotransmitter GABA were enriched in the upregulated genes at T3d and in the downregulated genes
258 at T14d (Supplementary Table 9).

259 At T14d, the composition of the biological processes to which the differentially expressed
260 genes contribute changed dramatically. In addition to the processes involving neuronal development,
261 cellular differentiation, and cellular communication that were already active at earlier time points (see
262 above), biological functions involving organ formation and system development such as embryo
263 morphogenesis (GO:0048598) and animal organ development (GO:0048513) now occurred. This
264 means that testosterone treatment causes a reorganization of the entire HVC (equivalent to an organ)
265 after about 14 days of treatment. The only process at the system/organ level that was triggered early,
266 immediately after the start of testosterone treatment, and continued throughout HVC development was
267 the development of the circulatory system (GO:0072359). This again underlines the importance of the
268 blood system both for the differentiation of cells/neurons and for the differentiation of the entire HVC
269 system. Among genes associated with ion transport (GO:0006811), which was enriched only at T14d,
270 genes encoded potassium ion channels especially those responsible for inward rectifying (such as
271 *KCNAB1*, *KCNJ3*, *KCNJ5*, *KCNJ8*, *KCNK10*, *KCNK16*, and *KCNK17*) were only upregulated at this
272 time point. Such genes are highly differentially expressed in the HVC of male zebra finches (Lovell et
273 al., 2013).

274 **Identification of key genes and gene networks for testosterone-induced anatomical and**
275 **behavioral changes.**

276 We used WGCNA (weighted gene correlation network analysis) (Langfelder and Horvath, 2008, 2012),
277 an unbiased clustering method, to identify functional units of gene co-expression networks relevant to
278 testosterone-induced morphological and behavioral changes. We constructed an overall gene network
279 composed of the HVC transcriptomes of testosterone-treated animals (Table 1). In the network, 12,360
280 genes were clustered into 14 modules by the WGCNA procedure (Fig. 4A and Supplementary Fig. 5).
281 After module identification, WGCNA integrates gene expression data with morphological (HVC
282 volume) and behavioral (song parameters) data to find modules that correlate strongly with the given
283 parameters.

284 The "turquoise" module (an arbitrary name given by the "WGCNA" R package) was
285 significantly and positively correlated with duration of testosterone implantation, HVC volume, song
286 rate, song length, and the number of syllables in a song (Fig. 4A and Supplementary Table 10). Seven
287 other modules were enriched for neuronal properties (Fig. 4B and Supplementary Table 11) and were
288 significantly correlated with at least two song-related parameters. For example, the member genes of
289 the "brown" module were enriched for "projection neuron", "myelin", "dendrite", and "spine", and
290 this module was negatively correlated with song length, the number of syllables per song, and syllable
291 repetition rate

292 The "turquoise" module was the biggest module with 6,480 member genes (Supplementary
293 Table 10) and with the greatest average intramodular connectivity among the 14 modules, meaning
294 members of this module are more likely to co-express than members of other modules (Supplementary
295 Fig. 5). GO-term enrichment analysis showed it was highly associated with anatomical structure
296 morphogenesis (GO:0009653, Bonferroni-adjusted P-value = 8.2×10^{-17}). Many genes of the
297 "turquoise" module have been associated with testosterone-induced angiogenesis and neuron
298 recruitment of HVC (Hartog et al., 2009; Kim et al., 2008; Louissaint et al., 2002; Rasika et al., 1999;

299 Rasika et al., 1994), including brain-derived neurotrophic factor (*BDNF*), vascular endothelial growth
300 factor (*VEGFA* and *VEGFC*) and VEGF receptors (*KDR, FLT1, FLT4*), insulin-like growth factor 1
301 (*IGF1*), and matrix metallopeptidases (*MMP2* and *MMP9*) (Fig. 4C and Fig. 2E). Chondroitin sulfate
302 proteoglycan 4 (*CSPG4*), the main component of perineuronal nets, has been associated with the
303 closure of the sensitive period of song development (Cornez et al., 2020). In addition, 20
304 steroidogenesis enzymes were members of this module, such as hydroxysteroid dehydrogenase
305 (*HSD3B2*), 17α-hydroxylase (*CYP17A1*), 17β-hydroxysteroid dehydrogenase (*HSD17B12*),
306 aromatase (*CYP19A1*) and 5α reductases 2 (*SRD5A2*), as well as steroid receptors such as estrogen
307 receptors (*ESR1* and *ESR2*), androgen receptor (*AR*), and G protein-coupled receptor family C group
308 6 member A (*GPRC6A*), which might mediate the non-genomic effects of androgens (Pi et al., 2010).
309 Thus, the unbiased clustering method, which integrates the transcriptomes with behavioral and
310 anatomical measurements under the influence of testosterone, was able to assign functionally relevant
311 genes into a module, even though most of the genes were transiently regulated. The very many genes
312 of the turquoise module were likely expressed in different cell types of HVC, including projection
313 neurons and interneurons, although the "turquoise" module failed to pass the threshold for cell-type
314 enrichment analysis (Fig. 4B).
315

316 **Transcription factor Sp8, a hub-gene.**

317 Transcription factors are among the top 10 most connected genes in 10 of the 14 modules. Of the
318 turquoise module, approximately 10% of the most connected genes (intramodular connectivity higher
319 than the 90th percentile) were transcription factors, and the most connected gene was *SP8*, a zinc-
320 finger transcription factor of the SP/KLF family. It is required for the survival of pallial progenitor
321 cells during corticogenesis (Limame et al., 2014; Zembrzycki et al., 2007), crucial in angiogenesis
322 (Safe and Kim, 2008), CNS development (Bell et al., 2003; Gaborieau et al., 2018), as well as adult
323 neurogenesis in mice (Waclaw et al., 2006). *SP8* was up-regulated after two weeks of testosterone

324 treatment, a time point when the regulated genes were highly associated with anatomical changes at
325 systemic levels (Fig. 2E and Fig. 3C).

326 To evaluate the probability of whether SP8 can directly regulate transcription of its fellow
327 members in the "turquoise" module, we assessed the presence of SP8 binding sites (V$SP1F) in the
328 promoter sequences of 1,151 genes with high intramodular connectivity with *SP8* (adjacency > 0.5)
329 using the "Genomatix-overrepresented TFBS tool". SP8 binding sites are enriched in the input
330 sequences and potentially exist in the promoter sequences of 625 genes, including *VEGFA* and *ESR2*
331 (Supplementary Table 12). Given that transcription factors can regulate gene expression in a
332 combinatorial fashion (Reményi et al., 2004), we proceeded to identify the potential interacting
333 partners of SP8 protein among the 1,151 genes with high intramodular connectivity with *SP8* using
334 the Search Tool for the Retrieval of Interacting Genes/Proteins (STRING) database. The database
335 identified 11 proteins that might physically interact with SP8 based on bioinformatics evidence
336 (Supplementary Fig. 6), including two transcription cofactors EED and SIN3A, and four transcription
337 factors; three of the four belong to the GATA family (*GATA2*, *GATA3,* and *GATA4*). We subsequently
338 evaluated the probability that SP8 forms a transcription factor complex with GATA using the
339 "Genomatix-overrepresented TFBS tool" module search function. Binding sites for complex
340 V$GATA-V$SP1F were enriched in the promoter sequences of the 1,151 genes and were potentially
341 present in 169 submitted genes, including *VEGFA* and *ESR2* (Supplementary Table 13).

342 The SP family plays an important role in estradiol-dependent gene regulation in breast cancer
343 cell lines (Safe and Kim, 2008) and the presence of estrogen receptors enhanced the binding of the SP
344 family (Fuentes and Silveyra, 2019). We thus investigated the promoter sequence of *SP8* for the
345 possibility of direct modulation of nuclear steroid receptors. The MatInspector tool of the Genomatix
346 software suite identified two potential EREs (V$ESR2.01) in the promoter of *SP8*, indicating the
347 possibility of direct modulation of ESR2. We observed colocalization of *SP8* and *ESR2* mRNA in
348 *SLC17A6* positive (glutamatergic) and some *SLC17A6* negative HVC cells (Fig. 5) by performing a

349 RNAScope® fluorescent multiplex assay in the HVC of T14d birds, a time point when *SP8* and *ESR2*
350 mRNA were both up-regulated detected by microarray (Fig. 2E). Ninety-six percent of *SP8* positive
351 cells were also *ESR2* positive; conversely, 97% of *ESR2* positive cells were *SP8* positive. *ESR2* has
352 not previously been found in the HVC of songbirds (Bernard et al., 1999), which may be due to its
353 transient expression after testosterone treatment. The fact that the two genes were expressed nearby in
354 the same cell may indicate physical interactions between the gene pair and warrant further
355 investigation into the nature of their relationship.

356 **Discussion**

357 We examined at several time points during testosterone-induced song development the progression of
358 transcriptomic changes in the song control nucleus HVC, in parallel with changes in HVC volume and
359 song in female canaries. The number of differentially expressed genes in the HVC of testosterone-song
360 induced female canaries is unprecedented compared to other brain areas of adult vertebrates. We found
361 that the HVC responded to testosterone within 1 hour with extensive changes in gene expression (2,652
362 genes) that preceded the earliest changes in song development. The genes that were differentially
363 expressed from T1h to T3d were mainly related to neuronal and cellular differentiation, including
364 angiogenesis. While gene regulation of neuronal/cellular processes continued throughout song
365 development, the extent of testosterone-related gene regulation extended slightly to nervous system
366 development at T7d (2,472 differentially expressed genes) and expanded massively to organ/system
367 (HVC) development at T14d (7,702 differentially expressed genes), consistent with the larger
368 delineable HVC and the organized song pattern at this stage. Intriguing, most extensive changes in
369 transcription occurred at the stage (T14d) when song pattern and HVC phenotype became most similar
370 to those of singing male canaries. Only 1.6% (153 genes) of the total 9,710 differentially expressed
371 genes were regulated at all time points from T1h to T14d, suggesting that the different developmental
372 stages of HVC and song differentiation require time-specific gene networks. The large number of
373 genes that could be directly regulated by androgen and estrogen receptors based on the sequence of

374 potential promoters, the presence of androgen and/or estrogen receptors in about 60-70% of all HVC
375 neurons (see below), as well as the increase in the expression of these receptors at T14d, speaks for
376 massive, parallel regulation of very many genes, including other transcription factors, in the HVC by
377 androgen and estrogen receptors.
378

379 **Fast, transient, and long-term constant regulation of large transcriptomes after**
380 **testosterone treatment.**

381 The HVC is a medium-sized brain area consisting of 30,000 to 50,000 cells, including neurons, glia,
382 and endothelial cells, expressing over 10,000 genes, accounting for about two-thirds of the (currently
383 known) protein-coding genes in the canary genome (Frankl-Vilches et al., 2015). In the canary HVC,
384 about 55% of cells express androgen receptors and about 25% express estrogen receptors (Gahr, 1990a,
385 b; Johnson and Bottjer, 1993, 1995), and some express both receptor types (Gahr, 1990b), which
386 suggest that about 60-70% of the HVC cells express androgen and/or estrogen receptors, making these
387 cell types direct targets for the action of testosterone and its metabolites. Local conversion of
388 testosterone to 5α-DHT and 17β-estradiol is possible due to the expression of 5α-reductase and
389 aromatase in HVC (this study; (Metzdorf et al., 1999)). Although we expected testosterone and its
390 metabolites to affect multiple gene networks with diverse cellular and biological functions, we were
391 surprised by the extensive transcriptional regulation and its rapidity. Based on previous
392 autoradiographic studies (Arnold et al., 1976; Marynick et al., 1976), testosterone takes about 30
393 minutes to reach the HVC after implantation. Thus, it is even more surprising that testosterone altered
394 the expression of more than 2,700 genes in an hour or less. This already large number of differentially
395 expressed genes after testosterone treatment remained at this level until about 14 days after treatment
396 when the number roughly tripled to 7,702 (Fig. 3A). Interestingly, the down-regulated genes increased
397 by 23.5% between the 7 and 14 days, while the up-regulated genes increased by 604.9%.

398 This rapid and extensive regulation of gene expression affecting many functions makes the
399 hypothesis of avalanche-like gene regulation in which androgen and estrogen receptors modulate the
400 expression of a few hub genes in many cells, which in turn regulate most other genes, improbable. *In*
401 *silico* analyses showed that androgen and estrogen binding sites are enriched in the promoter sequences
402 of T1h testosterone-sensitive genes, supporting the possibility of fast massive parallel gene regulation
403 by androgen and estrogen receptors. Chromatin immunoprecipitation studies found that the binding
404 sites occupied by androgen and estrogen receptors could be located up to 10 kb from the transcription
405 start sites, which is outside the genomic range we studied (Bourdeau et al., 2004; Takayama et al.,
406 2007; Wilson et al., 2016). Therefore, direct control of genes by androgen and estrogen receptors may
407 be even more extensive than suggested here. Nevertheless, androgen and estrogen receptors regulate
408 transcription factors within 1 hour that might amplify the androgen and estrogen receptor-mediated
409 testosterone-induced effects (**Fig. 3**A). This indirect control of gene expression by testosterone could
410 be very pronounced after 14 days of testosterone treatment when the expression of a large number
411 (730) of transcription factors changed. However, promoter analysis showed that genes with ARE and
412 ERE were similarly enriched in the transcriptomes of T1h and T14d (83.7 and 82.1 % of differentially
413 expressed genes, respectively) and affected about 25 % more genes at both time points than in
414 randomly selected gene pools of control HVCs. Single-cell transcriptomes would help clarify whether
415 and how testosterone regulates gene expression in cell types expressing or lacking androgen and/or
416 estrogen receptors.

417 The majority (52.3%) of the testosterone-sensitive HVC genes (4,798 of 9,710) were regulated
418 only at a single time point after testosterone administration, i.e. in a time-limited manner. This suggests
419 that certain gene networks are regulated by androgen and/or estrogen receptors at different time points
420 or are induced by previously regulated networks and no longer require testosterone. We did not
421 explicitly investigate the latter possibility. However, song development succumbs when testosterone
422 implants are removed (Vellema et al., 2019), implying that the presence of testosterone or its

423 metabolites is required for gene regulation throughout the song development. Because androgen- and
424 estrogen-receptor binding to DNA is highly tissue- and context-specific (Pihlajamaa et al., 2015;
425 Pihlajamaa et al., 2014), androgens and estrogens could regulate the expression of different genes at
426 different time points during HVC differentiation. Over 61% of the top ten GO terms across the sixtime
427 points examined are active as early as one hour after testosterone administration (Fig. 3C), suggesting
428 that although testosterone regulates certain cellular and biological functions more long-lasting, it
429 transiently determines the expression of most genes involved in these functions (Fig. 3B). The dynamic
430 and transient nature of HVC transcriptomes during song development reflects the observation that
431 different anatomical features of HVC neurons, glial cells, and vessels change in parallel with song
432 features at different time points ((Hartog et al., 2009; Louissaint et al., 2002; Nottebohm, 1980; Rasika
433 et al., 1994; Vellema et al., 2019) and this study) (see below).

434 The diverse and very extensive effects of testosterone on gene expression in HVC cells were
435 unexpected. Comparable studies of transcriptomic changes following testosterone treatment or
436 associated with seasonal phenotypes in birds, mammals, amphibians, and fish reported much less
437 differentially expressed genes, both in peripheral tissues (Cheviron and Swanson, 2017; Dopico et al.,
438 2015; Faber-Hammond et al., 2015; Morey et al., 2016; Sharma et al., 2019) and vertebrate brain areas
439 (Bao et al., 2019; Peterson et al., 2013; Zhang et al., 2016; Zhao et al., 2021). A comparably large
440 effect was only reported for seasonal changes in the testes (Tian et al., 2019). For most peripheral
441 tissues, this much smaller number of affected genes could be explained by a smaller number of cell
442 types that make up the organ compared to brain areas such as the HVC, which comprise a larger
443 number of different cell types (Colquitt et al., 2021). Alternatively, the enormous effect of testosterone
444 on the HVC transcriptome could be due to the expression of androgen and/or estrogen receptors in
445 about 60 to 70% of HVC neurons (Gahr, 1990a, b; Johnson and Bottjer, 1993, 1995) which should
446 include most HVC neuron types. The large number of testosterone-induced differentially expressed
447 genes in the adult canary HVC, especially at later stages (T14d) of song development, is reminiscent

448 of embryonic organ formation, which has also emerged as a central biological function in the GO
449 analysis (Fig. 3). This suggests that the testosterone (or estrogen)-triggered induction of adult
450 behaviors, such as parental behavior and courtship, requires a much more extensive reorganization of
451 the transcriptome and the associated biological functions of the brain areas involved than previously
452 thought. In this context, it should be noted that the HVC, although a central component, is only one
453 component of the song control system, and that singing requires the functionality of at least three brain
454 areas of the descending song motor system (Wild, 2004). Since these brain areas and the sound-
455 producing organ, too, express androgen receptors (Gahr and Wild, 1997; Godsave et al., 2002),
456 testosterone orchestrates the regulation of a large part of the canary gene pool to achieve singing.
457

458 **Testosterone-driven transcriptomic changes, neural changes, and song differentiation.**
459 The onset of singing was about 4 days. Then singing evolved from early sub-songs to late sub-songs
460 to plastic songs with increasing stereotypy of syllables, increasing syllable repetition rate, and
461 increasing total number of syllables strung together in a song (Fig. 1 and Supplementary Fig. **1**). There
462 is some individual variability in the transitions from early sub-songs to late sub-songs and plastic songs,
463 but songs uttered after 14 days resembled a typical canary song much more than songs uttered at earlier
464 time points after the start of testosterone treatment. Our experiment ended after 14 days with plastic
465 songs, already showing most of the characteristics of typical canary songs (long sequences, high
466 repetition rates, several different syllables in one song passage, short inter-syllable pauses). The
467 transcriptional changes on days 1 and 3, likely, prepare the HVC to produce early subsongs, those on
468 day 7 likely are relevant for singing late subsongs and contribute to differentiation processes of HVC
469 circuits required for the production of plastic songs, and transcriptional changes on day 14 are relevant
470 for the production of plastic songs, or for differentiation processes that lead to fully stereotyped songs
471 that emerge in general between 14 days to weeks of testosterone treatment (Vellema et al., 2019).

472 Most interesting, gene regulations related to certain functional processes are initiated fast after
473 testosterone treatment and last throughout the studied song development, while others show a late-
474 onset. Although this rapid transcriptional change at T1h produced homeostatic responses to reduce the
475 activity of testosterone, it also activated many genes of many different cellular and biological functions
476 - as shown in Gene Ontology (GO) analysis - that are involved in cellular plasticity, such as
477 cytoskeletal organization and in cellular morphogenesis (Fig. 3C). Next to targeting permanent neuron
478 populations of HVC (Gahr, 1990b), testosterone seems to affect angiogenesis, neurogenesis, and
479 gliogenesis (Goldman and Nottebohm, 1983; Louissaint et al., 2002). Concerning neuronal
480 development, the differentially expressed genes associated with "dendrites," "axon," and "spine" were
481 enriched after one hour of treatment, indicating the fast onset of neuronal differentiation (Fig. 3C, 3D).
482 In addition, the balanced activity of excitatory and inhibitory neurons in the HVC might be important
483 for HVC networks to become active in song control. Accordingly, we observed an enrichment of genes
484 associated with "glutamate" (downregulated) at early time points (T3h and T8h) and enrichment of
485 genes associated with "GABA" at T3d, when the first songs occurred (Fig. 3D). At the earliest stage,
486 the only system-level process that was initiated was vascular system development. The vascular
487 endothelial growth factor (*VEGF*) receptors, *KDR* and *FLT4*, were expressed at higher levels in T1h
488 animals than in controls (Fig. 2E). In addition, *FLT1* (another VEGF receptor) was upregulated at T8h
489 and *VEGFA* and *VEGFC* at T3d. At the system level, GO term analysis showed that differentially
490 expressed genes related to circulatory system development (GO:0072359) were enriched at all time
491 points starting at T1h while system (organ) development (GO:0048731, GO:0048513) concerning the
492 entire HVC was massively regulated at 14 days of treatment (Fig. 3C). Our results are consistent with
493 the previous finding that testosterone triggers the development of the vasculature in the HVC (Hartog
494 et al., 2009; Louissaint et al., 2002) and suggest that processes such as an expanded vasculature are
495 important for neuronal differentiation and increased neuronal activity. These cellular differentiation
496 processes, which begin in the first days of testosterone treatment, may contribute to the onset of song

497 pattern generation and precede the extensive systemic changes in the HVC of female canaries treated
498 with testosterone over an extended period (T14d).

499 In T7d when the canaries were just about to change from subsong to plastic song, i.e. song
500 stereotypy increased and more HVC typical functions such as syllable sequencing emerged,
501 transcription of genes associated with "endothelial cells" was enriched (Fig. 3D). Testosterone
502 metabolite 17β-estradiol (but not 5α-DHT) induces HVC endothelial cells to secrete VEGF, which
503 activates the VEGF signaling pathway and angiogenesis and releases BDNF (Louissaint et al., 2002).
504 BDNF mediates the recruitment and survival of adult-born neurons (Rasika et al., 1999) and was
505 upregulated at the T7d transcriptome. Genes related to neuronal differentiation are still differentially
506 expressed at T7d. In relation, the anatomy of the HVC is probably subject to continuous but subtle
507 morphological changes after testosterone levels are increased (see above), contributing to the
508 phenotype of the HVC. However, the resulting volume change in the T7d animals was statistically
509 indistinguishable from the control animals; only three T7d birds had an increased HVC volume
510 comparable to the T14d animals (Fig. 1F). It needs to be investigated which electrophysiological
511 properties of which HVC neurons change at this stage of song development.

512 In T14d, the anatomical appearance of the HVC has changed, making the HVC recognizable
513 in histological sections, resulting in an apparent enlargement of the HVC (Fig. 1F) (Gahr, 1990a; Gahr
514 and Metzdorf, 1997). The HVC volume of T14d birds was comparable to published data in which
515 female canaries were implanted with testosterone for three weeks or longer (Fusani et al., 2003; Hartog
516 et al., 2009; Madison et al., 2015; Nottebohm, 1980; Rasika et al., 1994). This change of phenotype of
517 the entire HVC correlates with massive changes in gene expression occurring during the second week
518 of testosterone treatment when approximately three times as many genes were differentially expressed
519 as at time T7d. Which neuroanatomical changes in detail contribute to the change in HVC phenotype
520 need to be seen but might involve many different processes as suggested by the massive increase in
521 differentially expressed genes and the stark increase of systems-level GO-terms. Concerning neuronal

522 differentiations relevant to the interconnection of neurons, the down-regulation of genes seems to be
523 more relevant than the up-regulation after 14 days of testosterone; genes associated with "spikes" were
524 even downregulated at all time points in our experiment (Fig. 3D) A recent study showed that dendritic
525 spine density in the HVC decreased after testosterone implantation, suggesting that synaptic pruning
526 occurs in the HVC and contributes to crystallization of the female canary song (Vellema et al., 2019).
527 The upregulation of ion channel genes such as inward rectifying potassium channels at 14 days of
528 treatment might stabilize the electrical properties of HVC neurons, which could reduce variability in
529 neuronal networks and therefore, result in the observed increased stability of song pattern at that stage.
530 The differentiation of HVC at the cellular and system levels at T14d is consistent with the marked
531 increase in song length and syllable rate between days 7 and 14. Longer songs mean that a greater
532 number of syllables are uttered sequentially without long pauses; a higher syllable rate means that
533 more syllables are sung per time, which requires a reduction in pauses between syllables and/or the
534 exclusion of long syllables. These song parameters reflect the sequential temporal organization of
535 syllables, which is a major function of HVC circuitry (Basista et al., 2014; Goldin et al., 2013;
536 Hahnloser et al., 2002). Alternatively, but not excluding the possibility, the enormous expansion of the
537 differentially expressed transcriptome of the HVC could be due to the increased singing activity of
538 T14d females. Singing increases the expression of the immediate early gene ZENK in canary HVC
539 (Jarvis and Nottebohm, 1997), which may regulate further gene cascades. Since ZENK expression
540 does not differ between T7d and T14d birds, we favor the hypothesis that the strong increase in
541 differentially expressed genes and thus biological processes in the HVC of T14d birds is related to
542 song differentiation processes rather than song activity.
543

544 **Conclusions.**

545 Testosterone treatment rapidly triggered extensive transcriptional changes in the HVC of female
546 canaries and dramatically altered song. After the rapid onset (1 hour or less) of the transcriptional

547 changes, the transcriptomes changed very extensively several times during the two-week evolution of
548 song. This progression of transcriptomes shows that most genes were regulated only at specific stages
549 of HVC and song development. The differentially expressed genes are associated with many different
550 biological functions, with systemic functions emerging primarily after prolonged testosterone
551 treatment. This suggests that adult song development requires a restructuring of the entire HVC,
552 including most HVC cell types, and not just a change in some neuronal populations or cellular
553 components. These changes seem driven by parallel direct regulation of thousands of genes by
554 androgen and estrogen receptors, as well as by other hub genes such as *SP8* that are themselves under
555 steroidogenic control. Our study identified vast gene networks that correlate highly with behavioral
556 and neuroanatomical changes during the song development of adult birds.
557

558 **Materials and Methods**

559 **Animals.**

560 Forty-seven adult female canaries were used in this study (see Table 1). Forty-two of these birds were
561 planned for microarray analysis, however, three of these birds were excluded since the RNA amount
562 or quality was not sufficient for the microarray hybridization. Adult female canaries (*Serinus canaria*,
563 at least one-year-old) were bred in the animal facility of the Max Planck Institute for Ornithology,
564 Seewiesen, Germany. Housing and welfare of the animals followed the European Directives for the
565 protection of animals used for scientific purposes (2010/63/EU), and protocols were approved by the
566 Government of Upper Bavaria under AZ-No. 55.2/54-2531-68/12. The sex of the animals was
567 confirmed by PCR using primers P2 and P8 for the CHD genes (Griffiths et al., 1998) and by visual
568 inspection of the female reproductive system after killing. Food and water were provided ad libitum at
569 all times. Birds were kept under local light conditions. Six to eight weeks before the experiment started
570 (beginning in September at the earliest), the light schedule was gradually changed to short-day

571 conditions (light: dark = 9:15 hours). After the birds became accustomed to the short-day light cycle,
572 singing was monitored. Birds were divided into a control group and six experimental groups; the
573 numbers of birds per group are summarized in Table 1. Testosterone was implanted into the
574 experimental groups for different periods (T1h, T3h, T8h, T3d, T7d, T14d, see Method: Testosterone
575 Implantation).
576

577 **Song monitoring.**

578 About 5% of female canaries sing spontaneously without hormone manipulation (Ko et al., 2020). To
579 ensure that vocal activity in our experiment was indeed triggered by testosterone implantation, birds
580 used in this study were housed alone in sound-attenuated boxes (70 × 50 × 50 cm) and all vocalizations
581 were recorded continuously for two weeks before testosterone implantation and until killing. The
582 microphone (TC20, Earthworks, Milford, New Hampshire) in each silenced box was connected to a
583 PR8E amplifier (SM Pro Audio, Melbourne, Australia) that fed into an Edirol USB audio recording
584 device (Edirol UA 1000, Roland, Los Angeles, California) connected to a computer. Vocalizations
585 were recorded at a sampling rate of 44.1 kHz and a resolution of 16 bits using Sound Analysis Pro
586 2011 software (Tchernichovski et al., 2000).

587 **Song analysis.**

588 Birds treated with testosterone began singing unstable so-called subsongs on average on day 4. Therefore, song
589 data refer to animals in the T7d and T14d groups. Nine hours of recordings were analyzed per day. We analyzed
590 all recordings from day 0 until the birds were killed (until the seventh or fourteenth day). For the analysis of
591 songs and song activity for the first 7 days, we combined data from T7d and T14d birds because their songs did
592 not differ significantly (Supplementary Fig. 3, Supplementary Table 2, and Supplementary Table 3). Song
593 analysis was performed using Multi_Channel_Analyser (MCA), a custom program with a graphical
594 user interface written in MATLAB (version R2016b, Mathworks), as described previously (Ko et al.,
595 2020) and available to the public (https://doi.org/10.5281/zenodo.1489098). Briefly, MCA loads song

596 files and generates sound spectrograms using the fast Fourier transform with a sliding time window of
597 294 samples and an overlap of 128 samples between adjacent sections. These settings result in a
598 spectrogram with a resolution of 150 Hz on the frequency axis and a resolution of 3.76 milliseconds
599 on the time axis. Due to background noise, syllable recognition was performed in three steps. First,
600 sound segments (songs and calls) were manually selected by visual inspection. Second, song segments
601 were selected if the sound segment was longer than 2 seconds. Third, syllables within the selected
602 segments were automatically detected using MCA by setting the following parameters in MCA: "High-
603 pass filter" to 2.0 kHz, "Threshold_wave_amplitude" to 0.001, and "Threshold_syllable_freq" to 50
604 Hz. Sounds shorter than 5 milliseconds (ms) were removed.

605 Digital samples of the recognized syllables were exported and used to calculate sound features.
606 As in the previous study (Ko et al., 2020), four song-level and four syllable-level parameters were
607 considered. Song-level parameters included three temporal features: Song length, number of syllables
608 in a song, syllable repetition rate, and a spectral feature, the slope coefficient (α) (Gardner, 1978;
609 Gisiger, 2001; Voss and Clarke, 1975). Syllable-level parameters include two temporal features,
610 syllable length and syllable spacing, and two spectral features, peak frequency, and Wiener entropy.
611 Song length was calculated by subtracting the timestamp at the end of the last syllable and the
612 timestamp at the beginning of the first syllable of a song. The syllable repetition rate was defined as
613 the number of syllables in the song divided by the song length in seconds. Syllable length was
614 calculated by subtracting the timestamp at the end of the syllable and the beginning of the syllable.
615 The interval between syllables was calculated by subtracting the timestamp at the beginning of the
616 following syllable and the end of the syllable. The peak frequency was the frequency at which the
617 power in the spectrogram of a syllable was highest. Wiener entropy is a unitless measure of signal
618 noise that provides a measure of the width and uniformity of the power spectrum. To obtain a broader
619 range, we used the log-transformed Wiener entropy. In this case, a Wiener entropy of 0 represents
620 white noise and the value infinity represents pure tone (Tchernichovski et al., 2000).

621 **Testosterone implantation.**

622 We custom-made the testosterone implants by packing testosterone (86500, Sigma-Aldrich, Saint
623 Louis, Missouri) into a 7-mm-long SilasticTM tube (Dow Corning, Midland, Michigan; 1.47 mm inner
624 diameter, 1.96 mm outer diameter, 0.23 mm thickness). Both ends of the SilasticTM tube were sealed
625 with silicone elastomer (3140, Dow Corning). After sealing, the implants were cleaned with 100%
626 ethanol to remove any testosterone particles. To ensure that no leakage occurred, the implants were
627 placed in ethanol in a fume hood overnight. Implants that were moist were discarded. One day before
628 implantation, implants were incubated overnight in 0.1 M phosphate-buffered saline (PBS) to ensure
629 the immediate release of testosterone upon implantation (Rasika et al., 1994). We started subcutaneous
630 implantation immediately after turning on the light at 8:30 am, with an interval of 20 minutes between
631 each bird, considering the time needed on the day of euthanasia. Control animals were implanted with
632 empty 7-mm silicone tubes that were also sealed with silicone elastomer. After the designated
633 implantation period (1h, 3h, 8h, 3d, 7d, or 14d, Table 1), the birds were killed with an overdose of
634 isoflurane, body weight was recorded, and the brains and oviducts were dissected, weighed, frozen on
635 dry ice, and stored at -80°C until further use. The testosterone implants were all present at the time of
636 euthanasia and held testosterone.

637 **Radioimmunoassay of plasma androgens.**

638 To confirm that systemic hormone manipulation increases circulating androgen levels, we performed
639 a radioimmunoassay on blood samples collected before and after testosterone implantation (Fig. 1A).
640 During the experiment, blood samples (approximately 100 µl) were collected twice from the wing vein
641 for testosterone analyses, once approximately 4 days before testosterone implantation, and once
642 immediately before killing. All blood samples were collected between 8 and 11 am, and within 3 min
643 to avoid handling effects (Wingfield et al., 1982). Blood samples were centrifuged (5,000 rpm, 10 min)
644 to separate plasma from blood cells. Testosterone metabolites in plasma were measured by
645 radioimmunoassay using a commercial antiserum to testosterone (T3-125, Endocrine Sciences,

646 Tarzana, California), as described previously (Goymann et al., 2002). Standard curves and sample
647 concentrations were calculated with Immunofit 3.0 (Beckman Inc. Fullerton, California) using a four-
648 parameter logistic curve fit and corrected for individual recoveries.

649 The testosterone concentrations were assayed in duplicates in four separate assays. The mean
650 extraction efficiency for plasma testosterone was 84.0 ± 6.8% (mean ± SD, N = 120). The lower
651 detection limits of the testosterone assays were 0.35, 0.34, 0.44, and 0.32 pg per tube, and all the
652 samples were above the detection limit. The intra-assay coefficients of variation of a chicken plasma
653 pool were 4.4%, 4.1%, 9.8%, and 2.6%. The inter-assay coefficient of variation as determined by the
654 variation of the chicken plasma pool between all the assays was 4.3%. The testosterone antibody used
655 shows significant cross-reactions with 5α-dihydrotestosterone (44%), our measurement might include
656 a fraction of 5α-DHT and thus we referred to the measurement as plasma androgen level.

657 Testosterone implants increased plasma androgen levels in all testosterone-treated groups
658 (Supplementary Table 2 and Supplementary Table 3). In contrast, pre-implantation levels were
659 statistically similar in all groups (159 ± 449 pg/ml, mean ± standard deviation (SD)). Implantation
660 increased plasma androgen levels by at least 28-fold above baseline (range: 17 to 88 ng/ml) after only
661 one hour. Plasma androgen levels after implantation for all testosterone-treated groups were not
662 statistically different from each other (plasma androgen levels after implantation for each group: CON
663 0.0472 ± 0.0240; T1h 46.9 ± 28.2; T3h 53.9 ± 14.8; T8h 35.6 ± 24.0; T3d 20.4 ± 4.47; T7d 14.8 ±
664 3.29; T14d 9.31 ± 2.94 ng/ml).

665 **Brain sectioning.**

666 Brains were sagittal sectioned using a cryostat (Jung CM3000, Leica, Wetzlar, Germany) in either 40
667 μm × 4 + 20 μm × 2 (N = 17) or 50 μm × 4 + 14 μm × 3 (N = 33) sections. The thick sections (40 or
668 50 μm) were mounted on glass slides for subsequent microdissection of the tissue for microarray
669 analysis, whereas the thin sections (20 or 14 μm) were mounted on RNase-free Thermo Scientific™
670 SuperFrost Plus™ slides (J1800AMNZ, Thermo Fisher Scientific, Waltham, Massachusetts) for Nissl

671 staining or RNAscope® in situ hybridization assay (Wang et al., 2012). All sections were stored at -
672 80 °C until further processing.

673 **Measurement of the HVC volume.**

674 A set of thin serial sections (20 or 14 µm) were Nissl-stained (0.1% thionine solution) and covered
675 with Roti-Histokitt II embedding medium (Roth). HVC areas were measured using ImageJ2 (Rueden
676 et al., 2017) (Fiji distribution (Schindelin et al., 2012)). All brains were coded so that the evaluators
677 had no information about the identity of individual brains and sections. Volumes were derived from
678 summed-area measurements multiplied by section thickness and section spacing.

679 **RNAScope® *in situ* hybridization assay.**

680 For RNAScope® *in situ* hybridization, three birds were used for a given probe at a given time point (3
681 slices for each bird). *In situ* hybridization for mRNA expression of *ALDH1A1*, *AR*, *HSD17B12*,
682 *SRD5A2*, and *UTS2B* was performed on sections (20 or 14 µm thick) using the RNAScope ®2.0 HD
683 Detection Kit (Advanced Cell Diagnostics, Newark, California) (Wang et al., 2012) according to the
684 protocols indicated by the manufacturer. Stained tissue sections were imaged using a Leica DM6000
685 B microscope (Leica). Quantification was performed using ImageJ2 (Fiji Distribution (Rueden et al.,
686 2017; Schindelin et al., 2012)). We measured the area of accumulated chromogenic particles in the
687 stained HVC sections for all probes and normalized the values using the area of the HVC region of the
688 same section. We used the Color Threshold function (color space: RGB; red channel: 0 to 47; green
689 channel: 0 to 165; blue channel: 0 to 160) to select the accumulated chromogenic particles and the
690 Analyze Particles function (minimum size = 8 μm^2) to count the number of accumulated chromogenic
691 particles and the area occupied by the chromogenic particles (user-defined macro file: "Marco_
692 quantify_density_singleProbes_quantify.ijm"). Our macro files are available at
693 https://github.com/maggieMCKO/TimeLapseTestoFemaleCanary/tree/main/RNAscopeQuantificatio
694 n.

695 RNAScope® fluorescent multiplex assay (Advanced Cell Diagnostics) was used to visualize
696 mRNA expression of *SP8*, *ESR2*, and *SLC17A6* following the protocols provided by the manufacturer.
697 Probes were conjugated to Atto 550 (*SP8*), Alexa 488 (*ESR2*), and Atto 647 (*SLC17A6*) fluorophores,
698 respectively. Sections were counterstained with DAPI. The stained tissue sections were imaged using
699 a Leica DM6000 B microscope.

700 **Microarray procedures and annotation.**

701 Thirty-nine adult female canaries were used for microarray analysis (see Table 1). The procedure was
702 described in (Ko et al., 2021). Briefly, for total RNA extraction, we dissected the HVC from the
703 abovementioned thick sections (40 or 50 μm), typically 24-32 slices per HVC, under a
704 stereomicroscope and transferred the tissue into an Eppendorf tube containing 340 μl of RLT buffer
705 mixture (containing DTT, Qiagen, Valencia, California). We used these rather thin sections for
706 dissection of HVC to avoid contamination of the samples with non-HVC tissues. RNA was then
707 extracted using the RNeasy® Micro Kit (Qiagen) with the optional DNase digest step. The RNA
708 quality was assessed using the Agilent Model 2100 Bioanalyzer (Agilent Technologies, Santa Clara,
709 California) and the RNA concentrations were assessed using a Nanodrop 1000 spectrometer (Thermo
710 Fisher Scientific). The RNA quality of all samples was of good quality (RNA integrity numbers (RIN)
711 > 7). The purified total RNA samples (at least 100 ng per sample) were subsequently processed and
712 hybridized using the Ambion WT Expression Kit (Thermo Fisher Scientific) and the Affymetrix WT
713 Terminal Labeling and Controls Kit (Thermo Fisher Scientific). The resulting cDNA was hybridized
714 to the Custom Affymetrix Gene Chip® MPIO-ZF1s520811 Exon Array, which has been used and
715 validated in successfully cross-species (zebra finches and canaries) hybridization studies (Dittrich et
716 al., 2014; Frankl-Vilches et al., 2015). Hybridization was performed for 16 hours at 45°C and 60 rpm
717 in the GeneChip Hybridization Oven 640. The arrays were washed, stained, and scanned using the
718 Affymetrix GeneChip Fluidics Station 450 and Affymetrix GeneChip scanner 3000 7G. The CEL files
719 were generated using Affymetrix GeneChip Command Console® Software (AGCC), and for quality

720 control, the success of individual hybridizations was assessed using the Affymetrix Expression
721 Console™ software. The 5.7 million male zebra finch-specific probes spotted on our custom array
722 correspond to approximately 4,711,133 probe sets and hence to 25,816 transcripts published in public
723 databases (NCBI and Ensembl) (Warren et al., 2010). We annotated more than 90% of the transcripts
724 to 12,729 human orthologous genes using publicly available databases (Ensembl, GenBank, UniProt,
725 and DAVID (Benson et al., 2005; Consortium, 2015; Flicek et al., 2014; Huang et al., 2008, 2009;
726 Yates et al., 2016)), as well as commercial databases (v 21 El Dorado, Genomatix, Precigen
727 Bioinformatics Germany GmbH (PBG), Munich, Germany). The microarray data generated in this
728 study have been deposited in NCBI's Gene Expression Omnibus (Edgar et al., 2002) and are accessible
729 through the GEO Series accession number GSE118522.

730 **Analysis of differentially expressed genes.**

731 ChipInspector software (v21, El Dorado Database vE28R1306, (Genomatix), Precigen Bioinformatics
732 Germany GmbH (PBG)) was used to calculate differential expression between each experimental
733 group and the control group. ChipInspector is a single probe-based analysis tool for microarray data
734 that increase sensitivity compared to conventional probe-set-based analyses, such as robust multi-array
735 analysis (Cohen et al., 2008; Tusher et al., 2001). We used the following parameters in ChipInspector:
736 group-wise exhaustive comparison: Delta threshold (controlling false positive rate) was set at 0; the
737 minimum coverage for each transcript was set at 10 significant probes; the minimum differential
738 expression was $|\log_2(\text{fold change})| \geq 0.5$. The significantly differentially expressed transcripts obtained
739 were annotated to human orthologous genes as described above. For transcripts belonging to the same
740 genes, the average expression was calculated if all transcripts were regulated in the same way (e.g., all
741 up-regulated or all down-regulated). If a gene contains both up- or down-regulated transcripts,
742 transcripts of the minority direction were discarded (<40% of the total transcripts), and the average
743 expression was instead calculated from the remaining transcripts (60% or more). Transcripts without
744 human orthologous gene annotation were removed before subsequent analyses.

745 The differential analysis results agree with the published data at the overlapping time point
746 (T14d, Fig. 2E): after two weeks of testosterone implantation, elevated mRNA levels of a vascular
747 endothelial growth factor receptor (*KDR*) and brain-derived neurotrophic factor (*BDNF*) were reported
748 (Louissaint et al., 2002). For further verification of the microarray results, we conducted RNAScope®
749 *in situ* hybridization assay for several genes involved in testosterone metabolism, including androgen
750 receptor (*AR*), 17β-hydroxysteroid dehydrogenase (*HSD17B12*), 5α reductases 2 (*SRD5A2*), and
751 aldehyde dehydrogenase 1 family member A2 (*ALDH1A2*) (Wang et al., 2012). The quantifications
752 were congruent with the microarray results (Fig. 2).

753 **Analysis of overrepresented transcription factor binding sites.**

754 We extracted 1,000 bp of genomic sequence upstream of the putative transcription start site as the
755 promoter sequence of a given gene from the canary genome (Frankl-Vilches et al., 2015; http://public-
756 genomes-ngs.molgen.mpg.de/cgi-bin/hgGateway?db=serCan1). We used the "Toolbox for
757 Overrepresented Transcription Factor Binding Sites" of the Genomatix software suite from Precigen
758 Bioinformatics Germany GmbH (Cartharius et al., 2005; Genomatix; Quandt et al., 1995; Sui et al.,
759 2005) to search for transcription factor binding sites (TFBSs) and determine whether individual TFBSs
760 (or TFBS pairs) were overrepresented in the input sequences against a user-defined background
761 (Genomatix). For each analysis, we drew a random sample of canary promoter sequences with the
762 number corresponding to the input and used the random sample as the user-defined background. For
763 the analysis of androgen and estrogen response elements (AREs and EREs), we extracted the promoter
764 sequences of the testosterone upregulated genes and the promoter sequences of the direct neighbors of
765 *SP8* identified by WGCNA (adjacency > 0.5). To assess the likelihood that SP8 forms a transcription
766 factor complex with GATA (the TF binding sites within 10 to 50 bp (center to center) of each other),
767 we used the module search function of the TFBS-Genomatix toolbox above. This analysis was
768 performed using zebra finch promoters as background because the option of using a custom
769 background (an equivalent size to the samples described above) was not available.

770 **Enrichment analysis of Gene Ontology (GO)-terms.**

771 We used ClueGO v2.5.0, an application developed under the Cytoscape environment v3.5.1 (Bindea
772 et al., 2009; Shannon et al., 2003), to predict the putative biological functions of genes of interest. This
773 software performs hierarchical analyses of GO term enrichment and fuses GO terms of similar
774 functions. Enrichment was determined with a right-sided test and corrected with the Bonferroni step
775 method considering multiple comparisons. Results were plotted using the R package ggplot2
776 (Wickham, 2009).

777 **Enrichment analysis of genes related to cell types, neuronal processes, and**
778 **neurotransmitters.**

779 We searched 33 terms associated with cell types, neuronal protrusion types, and biosynthesis of
780 neurotransmitters and neurotransmitter receptors and downloaded the gene lists associated with each
781 search term (Supplementary Table 8), using the "Genes and gene products" tool of the AmiGO 2
782 database (v2.4.26, release date 2017-07-05 (Ashburner et al., 2000; Consortium, 2017)). Subsequently,
783 we used the Fisher's exact test ("Fisher-Test", alternative hypothesis set to "greater") to determine
784 whether enrichment of a search term (genes associated with the term) is observed in the list of
785 differentially expressed genes of a given time point. We used the 15,609 protein-coding genes of the
786 canary as the universe in the Fisher's exact test (https://www.ncbi.nlm.nih.gov/genome/
787 annotation_euk/Serinus_canaria/101/#FeatureCountsStats). The P-values were adjusted for multiple
788 comparisons by Bonferroni's method using the "p.adjust" function. We performed the calculations in
789 R (Team, 2020) and visualized the results using the ggplot2 R package (Wickham, 2009).

790 **Weighted gene co-expression network analysis (WGCNA).**

791 WGCNA R package v1.51 (Langfelder and Horvath, 2008, 2012) was used to identify functional units
792 of gene co-expression network that are relevant for the testosterone-induced morphological and
793 behavioral changes (traits, Fig. 4A). WGCNA calculates the network adjacency matrix based on the

794 correlation of gene expression data and assigns genes into modules (sub-networks within the overall
795 network) based on the topological overlap matrix from a given network adjacency matrix. The
796 adjacency value can be seen as a proximate indicator for connection strengths among the nodes (genes)
797 in the network: a pair of highly correlated genes have an adjacency value of 1, indicating the pair is
798 likely co-expressed at a given time. After module identification, WGCNA integrates the gene
799 expression data with the morphological and behavioral data to identify modules strongly correlated
800 with specific parameters. A total of 32 traits were included in this study, and median and inter-quartile
801 range (Iqr) were calculated for each trait at the bird level. In co-expression networks, genes are seen
802 as "nodes" and "edges" (or connection strengths) between nodes are determined by the pairwise
803 correlations between gene expression profiles.

804 Before network construction, we calculated the normalized expression of the (Genomatix) CEL
805 files using the "justRMA" function in the "affy" R package v1.66.0 (Gautier et al., 2004). We followed
806 the suggestion of the authors of the WGCNA R package using the "collapseRows" function in the
807 WGCNA R package to aggregate gene expression data to gene level (Miller et al., 2011). We
808 constructed a signed hybrid network composed of all HVC samples (n = 39, Table 1) using the
809 "adjacency" function (type: "signed hybrid"). The soft thresholding power for the construction of the
810 adjacency matrix was set at 6 judging from the fitted curves calculated by the "pickSoftThreshold"
811 function. The adjacency value has a range from zero to one. The calculated adjacency matrix was fed
812 to the "TOMsimilarity" function to calculate the topological overlap matrix. Then, we used the
813 "cutreeDynamic" function to cluster genes into modules (sub-networks within the overall network)
814 based on the topological overlap matrix (the "TOMsimilarity" function). We used a minimum module
815 size of 100 genes and the "deepSplit" was set to four. We merged similar modules using the
816 "mergeCloseModules" function ("cutHeight" was set to 20%). Module Eigengenes is the first principal
817 component of a module's gene expression profile, a method of summarizing an entire module in one
818 vector (Burkett et al., 2018; Langfelder and Horvath, 2008, 2012). We calculated Module Eigengenes

819 using the "moduleEigengenes" function and calculated the correlation matrix between the Module
820 Eigengenes and the traits using the "cor" function (Pearson) in R (Team, 2020). Gene significance is
821 the Pearson correlation between a gene's expression profile and the traits (Burkett et al., 2018;
822 Langfelder and Horvath, 2008, 2012). The overall network connectivity, intramodular, and
823 intermodular connectivity were calculated using the "intramodularConnectivity" function in the
824 WGCNA package. The adjacency matrix was exported using the "exportNetworkToCytoscape"
825 function with a cutoff of 0.5 and was used for extracting the direct neighbors of *SP8*. The interactions
826 between *SP8* and its direct neighbors were evaluated using the Search Tool for the Retrieval of
827 Interacting Genes/Proteins database (STRING, v10.5 (Szklarczyk et al., 2015)). The interactions with
828 moderate confidence were retained (combined score greater than 0.4) and were visualized using
829 Cytoscape environment v3.5.1 (Bindea et al., 2009; Shannon et al., 2003).

830 **Experimental design and statistical analysis.**

831 All statistical analyses were performed in R (Team, 2020). For statistical comparisons of plasma
832 androgen levels, song features, and quantification of RNAScope® *in situ* hybridization, we used linear
833 mixed-effect models to analyze the fixed effects using the packages 'lme4' (Bates et al., 2014) and
834 'arm' (Gelman and Su, 2018) in a Bayesian framework with non-informative priors. We assumed a
835 Gaussian error distribution and confirmed that model assumptions were met by visual inspection of
836 model residuals. Plasma androgen levels, daily song rate, song length, and syllable repetition rate were
837 log-transformed, while the normalized stained HVC areas (RNAScope®) were square root
838 transformed. Subsequently, we simulated 10,000 times the estimates from the joint posterior
839 distribution of the model parameters using the 'sim' function and extracted the 95% credible intervals
840 (CrI) of the mean of the simulated values, which represent the uncertainty of the estimates (Gelman
841 and Hill, 2006). We considered an effect to be statistically meaningful when the estimated CrI did not
842 include zero or when the posterior probability of the mean of the difference between compared
843 estimates was higher than 0.95 (for more details on statistical inference see (Korner-Nievergelt et al.,

844 2015)). Linear mixed-effect models, model estimates, and posterior probability of comparisons were
845 given in Supplementary Table 2 and Supplementary Table 3. For visualization, we plotted the
846 predicted estimate from the models, the 2.5% and 97.5% CrI, as well as the raw data. Statistically
847 meaningful differences between compared groups can be inferred if the CrI of one group does not
848 overlap with the mean estimate of the other.

849 **Acknowledgments.**

850 We thank Dr. Stefan Leitner for providing breeding canaries, Roswitha Brighton and David Witkowski
851 for maintaining the colony, and Dr. Wolfgang Goymann and Monika Trappschuh for
852 radioimmunoassay of plasma androgens. Furthermore, we express our appreciation to Drs. Maude
853 Baldwin, Falk Dittrich, Vincent Van Meir, and Michiel Vellema for their comments on previous
854 versions of this manuscript and to the International Max Planck Research School for Organismal
855 Biology for training and support.

856 **Competing interests**

857 The authors declare no competing financial interests.

858

859 **Figure legends**

860 **Fig. 1. Testosterone implantation increased blood androgen levels, affects the HVC morphology,**
861 **and affects the song syntax of adult female canaries. A**, illustration of experimental procedures.
862 One blood sample was taken from each bird before implantation (blue shaded box) and one at the time
863 of sacrifice (orange vertical bars). CON: birds treated with empty implants; T: birds treated with
864 testosterone-filled implants for 1 hour (T1h), 3hours (T3h), eight hours (T8h), 3 days (T3d), seven
865 days (T7d), and fourteen days (T14d). **B**, testosterone implantation increased the androgen
866 concentrations in blood plasma significantly at all time points. Each color-coded dot represents one
867 measurement, before (blue) and after (orange) implantation. The black dots indicate the predicted
868 estimates of the linear mixed-effects models, and the vertical orange bars indicate the 95% credibility
869 intervals (CrI) of the predicted estimates. See Supplementary Tables 2 and 3 for the values of the linear
870 mixed-effects models and posterior probabilities. **C**, the daily singing activity of T7d and T14d groups
871 (measured by the percentage of time spent singing within nine hours in a day) significantly increased
872 twice on day 2 and day 10 (see also Supplementary Fig. 3). Each grey dot is one bird. **D**, Song length
873 in seconds (s) of T7d and T14d groups. Song length significantly increased daily until day 7 and further
874 increased on day 11. **E**, the number of syllables per song of the T7d and T14d groups increased
875 significantly daily after implantation. **F**, syllable repetition rate as syllables per second (sys/s) of the
876 T7d and T14d groups significantly increased on day 2 and day 9. In D-F, each gray dot represents a
877 measurement originating from one song. In C-F, black dots indicate the predicted estimates of the
878 linear mixed-effects models, and vertical orange bars indicate the 95% credibility intervals (CrI) of the
879 predicted estimates. See Supplementary Table 2 and Supplementary Table 3 for the estimates of the
880 linear mixed-effects models and the posterior probabilities. **G**, HVC volumes of T14d were
881 significantly different from that of control, T 3h, and T8h groups. The boxes indicate the
882 25th/50th/75th percentiles (bottom/middle/top bar), and the extent of the whiskers indicates the most

883 extreme values within 1.5 times of the inter-quartile range (IQR) of the hinge. Outliers are labeled in
884 red. *: Holm-adjusted P-value <0.05 (Kruskal-Wallis rank sum test followed by Dunn's post hoc test).
885

886 **Fig. 2. Validation of mRNA expression of five genes differentially expressed in the microarrays**
887 **using RNAScope® *in situ* hybridizations of HVC sections. A**, schematic of the songbird brain with
888 song control areas (white) including the HVC. **B** and **C**, representative photomicrographs of *in situ*
889 hybridizations of androgen receptor (*AR*) mRNA in B and 5α-reductase (*SRD5A2*) mRNA in C from
890 controls (CON) and testosterone-treated (T8h resp. T14d) birds. *AR* mRNA expression is increased in
891 the HVC of T14d (B, arrowheads) and *SRD5A2* mRNA is increased in the HVC of T8h animals (C,
892 arrowheads). **D**, testosterone increased the expression of genes in the HVC compared with controls
893 (e.g., *AR*, *SRD5A2*, *UTS2B*), and the expression of many genes differed between time points after
894 testosterone treatment started (e.g., *ALDH1A2*, *HSD17B12*). The *in situ* hybridization data of the five
895 depicted genes confirmed the statistical differences (Supplementary Table 2 and Supplementary Table
896 3) observed in the microarray-derived expression measurements (see Fig. 2E). Data represent the
897 proportion of the labeled HVC area (RNAscope staining of gene mRNA, see B and C) relative to the
898 total HVC area of that section. Each gray dot represents the value of one HVC section. Black dots
899 indicate the predicted estimates of the linear mixed-effects models, and vertical orange bars indicate
900 the 95% confidence intervals (CrI) of the predicted estimates. N = 3 birds per group. *ALDH1A2*:
901 aldehyde dehydrogenase 1 family member A2; *AR*: androgen receptor; *HSD17B12*: 17β-
902 hydroxysteroid dehydrogenase; *SRD5A2*: 5α-reductases 2; *UTS2B*: urotensin 2B. **E**, a heat map
903 showing the expression levels of selected groups of genes during testosterone treatment as compared
904 to the control HVCs ($\log_2$ fold change): genes of gonadal steroid receptor genes (blue), genes with
905 known functions in steroidogenesis (gray), genes involved in testosterone-induced angiogenesis (red),
906 genes involved in neuronal recruitment (green), and the gene encoding transcription factor *SP8*
907 (yellow).

908

909 **Fig. 3. Testosterone rapidly and persistently altered gene expression patterns in the HVC. A**,
910 number of differentially expressed genes in the HVC of testosterone-treated birds compared with
911 controls. The proportions of transcription factors (TF) were indicated in darker orange (upregulated
912 genes) and darker purple (downregulated genes). Already within one hour (T1h) more than 2,500 genes
913 were up- or down-regulated. A massive increase in gene regulation occurred 14 days (T14d) after
914 testosterone implantation. **B**, Only a small number of genes (1.6%) were differentially expressed at all
915 time points. We classified the differentially expressed genes into four classes based on their temporal
916 regulation patterns: 1) genes that are constantly upregulated, 2) genes that are constantly
917 downregulated, 3) dynamically regulated genes that are upregulated or downregulated at all six time
918 points, and 4) genes that are altered in expression at least at one but not at all time points compared
919 with controls (see Supplementary Table 4). **C**, GO term enrichment analysis of biological processes
920 involving differentially expressed genes during progressive testosterone action on HVC. The ten most
921 likely GO terms (based on Bonferroni-adjusted P-values) were displayed for each time point and
922 classified into six functional categories. The number of genes observed (cumulative across time points)
923 was presented in a stacked bar graph (see Supplementary Table 7 for full results). Biological processes
924 at the cell and neuron level occur early (1 hour), whereas those at the organs/system level, such as the
925 HVC as a network, occur late (14 days). **D**, enrichment analyses focusing on genes associated with
926 brain cell types (upper panels) and genes associated with neuronal features (types of neuronal
927 protrusions, genes involved in neurotransmitter biosynthesis, and genes encoding neurotransmitter
928 receptors, lower panels). Gray-filled cells were not significant (Fisher's exact test, P-values corrected
929 by FDR method). Full results are shown in Supplementary Table 8.

930

931 **Fig. 4. Identification of key genes relevant for testosterone-driven changes. A**, the unsupervised
932 clustering method WGCNA classified testosterone-regulated genes into 14 modules (named as color;
933 the number indicated the number of genes of each module) and associated these modules with
934 physiological traits (plasma testosterone concentration (T), body weight in g, brain weight in mg,
935 oviduct weight in mg, HVC volume in mm^3) and song measurements (song rate, song length, syllables
936 per song, syllable repetition rate, syllable length, syllable interval, maximum frequency, Wiener
937 entropy, and song slope. Note that certain gene modules are mainly positively correlated (red cells),
938 while other modules are mainly negatively correlated with physiological and behavioral parameters.
939 Pearson's r is given in a diagram cell (upper value) if the correlation was significant; the lower value
940 is the Bonferroni-adjusted P-value. The numbers next to the module names are the numbers of genes
941 included in the modules. **B**, analysis of gene enrichment in the 14 modules related to cell types
942 (oligodendrocyte, projection neuron) and neuronal parameters (axon, myelin, dendrite, spine) show
943 that eight modules are associated with neuronal properties. Gray-filled cells were not significant
944 (Fisher's exact test, P-values corrected by FDR method). See Supplementary Table 11 for full results.
945 **C**, a circos plot illustrates the entire WGCNA gene coexpression network by placing the 14 modules
946 (color-coded) at the outer edge of the circle. Intramodular connectivity is shown in gray; the
947 coexpression network of *SP8*, a zinc finger transcription factor, is shown in blue. *SP8* was the gene
948 with the highest number of coexpressed genes in the "turquoise" module. The genes of each module
949 were sorted in descending order by the number of neighbors of each gene (the height of the light orange
950 lines between the outer edge and the inner circle of intramodular connectivity).
951

952

953 **Fig. 5. The transcription factor *SP8* gene is frequently coexpressed with the estrogen receptor ß**
954 **gene (*ESR2*) in HVC cells.** Photomicrographs of RNAScope® fluorescence multiplex *in situ*
955 hybridizations of the HVC from T14d animals. Colocalization of *SP8* mRNA and *ESR2* mRNA in
956 both *SLC17A6* expressing (glutamatergic) neurons (A_1 to A_5) and *SLC17A6* negative neurons (B_1 to
957 B_3). Ninety-six percent of *SP8* positive cells were also *ESR2* positive; among SP8 and ESR2 double-
958 labeled cells, 60% were in *SLC17A6* expressing neurons. Scale bars in both top and bottom panels
959 correspond to 50 µm. *SLC17A6*: Solute Carrier Family 17 Member 6, formerly known as vGluT2.

960

961 **Fig. 6.** The timeline of the differentiation of organizational levels of HVC derived from transcriptome
962 data, HVC morphology measured as volume, and song activity and song syntax measurements after
963 testosterone treatment. The intensities of colors indicate the abundance of the features. Note that the
964 abundance of biological processes related to the circulatory system and neuron development precedes
965 that related to the nervous system development of HVC and precedes the emergence of song. The
966 emergence of a canary typical song pattern coincides with the system development of HVC. HVC
967 morphology (volume) maturated only after about 2 weeks of treatment, coinciding with the most
968 differentiated song patterns uttered by the canaries.

969

970 **Figures**

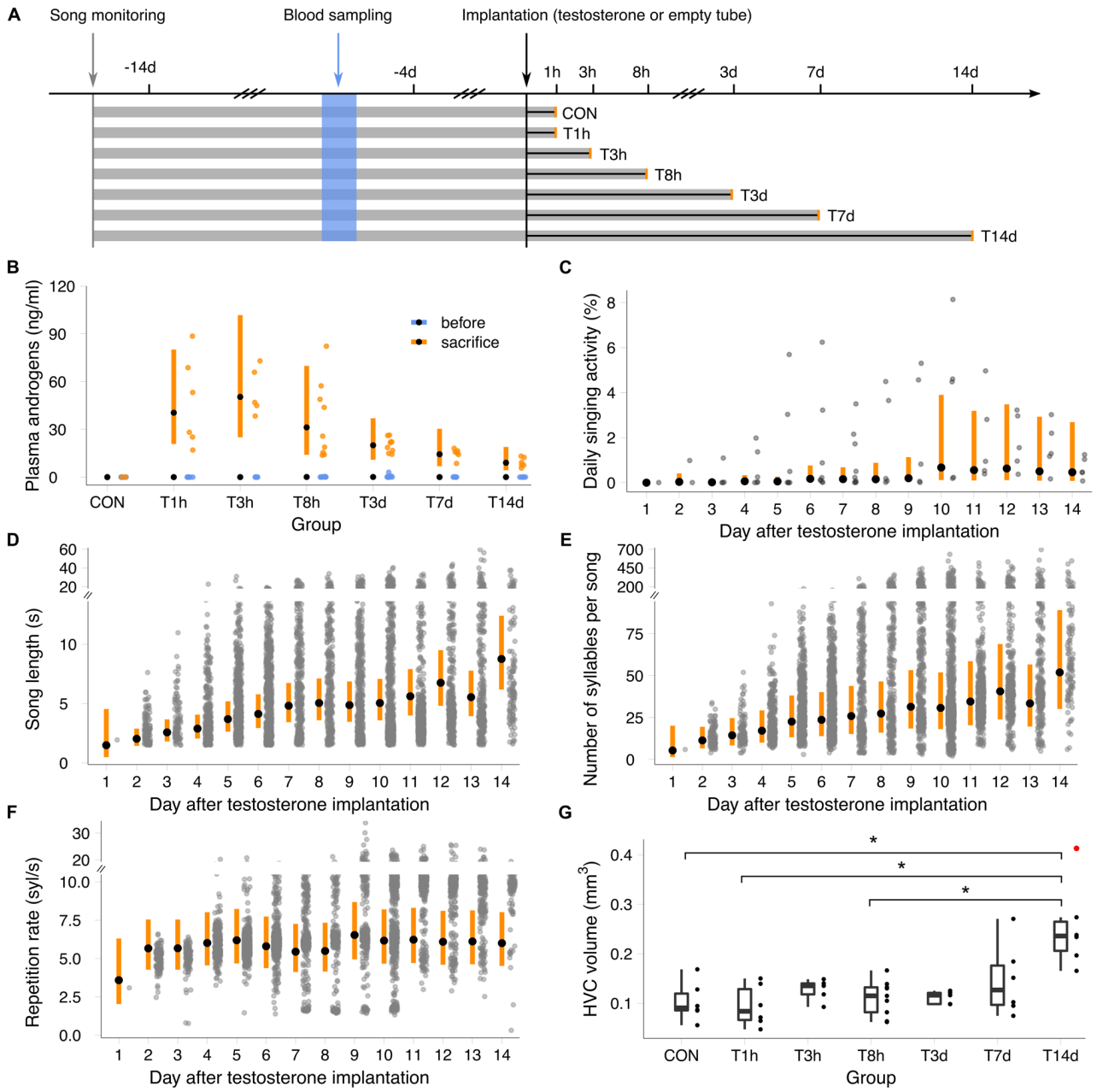

971

972 **Fig. 1.**

973

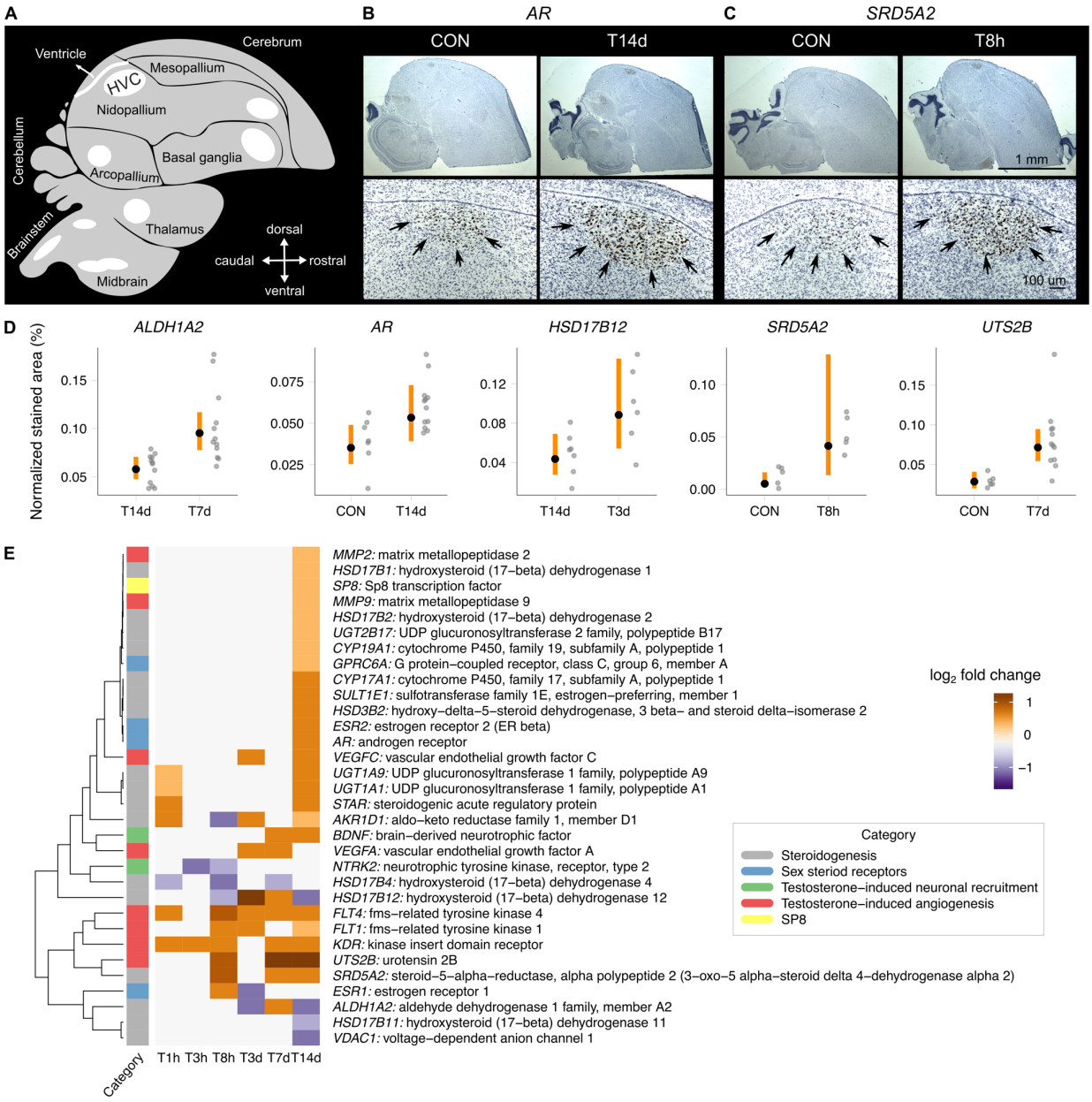
A
Ventricle
Cerebrum
Mesopallium
HVC
Nidopallium
Cerebellum
Basal ganglia
Arcopallium
Brainstem
Thalamus
Midbrain
dorsal
caudal
rostral
ventral
B
AR
CON
T14d
C
SRD5A2
CON
T8h
1 mm
100 um
D
ALDH1A2
AR
HSD17B12
SRD5A2
UTS2B
Normalized stained area (%)
T14d
T7d
CON
T14d
T14d
T3d
CON
T8h
CON
T7d
E
MMP2: matrix metallopeptidase 2
HSD17B1: hydroxysteroid (17–beta) dehydrogenase 1
SP8: Sp8 transcription factor
MMP9: matrix metallopeptidase 9
HSD17B2: hydroxysteroid (17–beta) dehydrogenase 2
UGT2B17: UDP glucuronosyltransferase 2 family, polypeptide B17
CYP19A1: cytochrome P450, family 19, subfamily A, polypeptide 1
GPRC6A: G protein–coupled receptor, class C, group 6, member A
CYP17A1: cytochrome P450, family 17, subfamily A, polypeptide 1
SULT1E1: sulfotransferase family 1E, estrogen–preferring, member 1
HSD3B2: hydroxy–delta–5–steroid dehydrogenase, 3 beta– and steroid delta–isomerase 2
ESR2: estrogen receptor 2 (ER beta)
AR: androgen receptor
VEGFC: vascular endothelial growth factor C
UGT1A9: UDP glucuronosyltransferase 1 family, polypeptide A9
UGT1A1: UDP glucuronosyltransferase 1 family, polypeptide A1
STAR: steroidogenic acute regulatory protein
AKR1D1: aldo–keto reductase family 1, member D1
BDNF: brain–derived neurotrophic factor
VEGFA: vascular endothelial growth factor A
NTRK2: neurotrophic tyrosine kinase, receptor, type 2
HSD17B4: hydroxysteroid (17–beta) dehydrogenase 4
HSD17B12: hydroxysteroid (17–beta) dehydrogenase 12
FLT4: fms–related tyrosine kinase 4
FLT1: fms–related tyrosine kinase 1
KDR: kinase insert domain receptor
UTS2B: urotensin 2B
SRD5A2: steroid–5–alpha–reductase, alpha polypeptide 2 (3–oxo–5 alpha–steroid delta 4–dehydrogenase alpha 2)
ESR1: estrogen receptor 1
ALDH1A2: aldehyde dehydrogenase 1 family, member A2
HSD17B11: hydroxysteroid (17–beta) dehydrogenase 11
VDAC1: voltage–dependent anion channel 1
T1h T3h T8h T3d T7d T14d
Category
log2 fold change
Category
Steroidogenesis
Sex steriod receptors
Testosterone–induced neuronal recruitment
Testosterone–induced angiogenesis
SP8

Fig. 2.

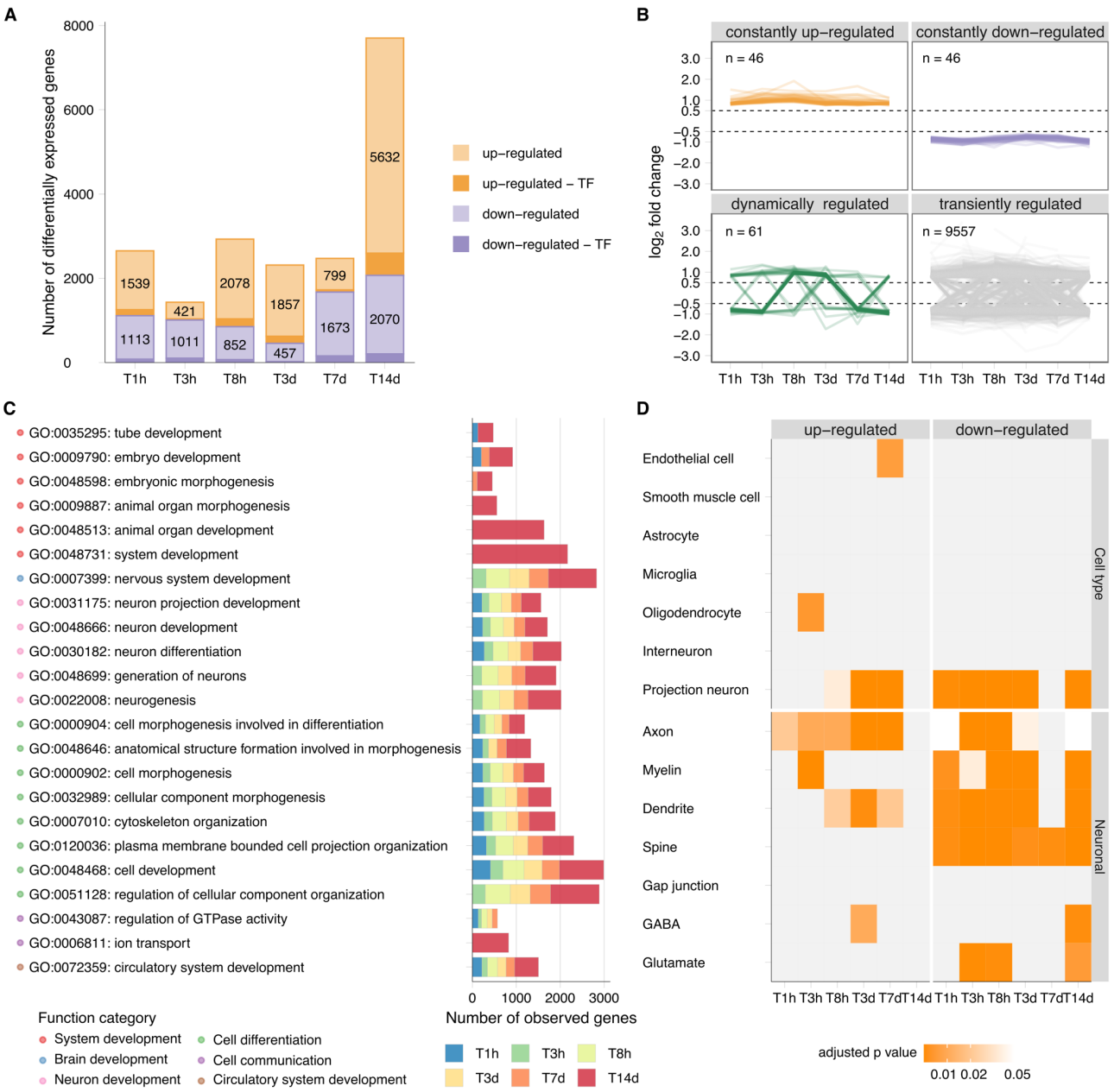
A
Number of differentially expressed genes
8000
6000
4000
2000
0
1539
1113
421
1011
2078
852
1857
457
799
1673
5632
2070
T1h
T3h
T8h
T3d
T7d
T14d
up−regulated
up−regulated − TF
down−regulated
down−regulated − TF
B
constantly up−regulated
constantly down−regulated
dynamically regulated
transiently regulated
n = 46
n = 46
n = 61
n = 9557
log2 fold change
3.0
2.0
1.0
0.5
−0.5
−1.0
−2.0
−3.0
T1h T3h T8h T3d T7d T14d
C
GO:0035295: tube development
GO:0009790: embryo development
GO:0048598: embryonic morphogenesis
GO:0009887: animal organ morphogenesis
GO:0048513: animal organ development
GO:0048731: system development
GO:0007399: nervous system development
GO:0031175: neuron projection development
GO:0048666: neuron development
GO:0030182: neuron differentiation
GO:0048699: generation of neurons
GO:0022008: neurogenesis
GO:0000904: cell morphogenesis involved in differentiation
GO:0048646: anatomical structure formation involved in morphogenesis
GO:0000902: cell morphogenesis
GO:0032989: cellular component morphogenesis
GO:0007010: cytoskeleton organization
GO:0120036: plasma membrane bounded cell projection organization
GO:0048468: cell development
GO:0051128: regulation of cellular component organization
GO:0043087: regulation of GTPase activity
GO:0006811: ion transport
GO:0072359: circulatory system development
0
1000
2000
3000
Number of observed genes
Function category
System development
Brain development
Neuron development
Cell differentiation
Cell communication
Circulatory system development
T1h
T3h
T8h
T3d
T7d
T14d
D
up−regulated
down−regulated
Endothelial cell
Smooth muscle cell
Astrocyte
Microglia
Oligodendrocyte
Interneuron
Projection neuron
Axon
Myelin
Dendrite
Spine
Gap junction
GABA
Glutamate
Cell type
Neuronal
T1h T3h T8h T3d T7dT14d T1h T3h T8h T3d T7dT14d
adjusted p value
0.01 0.02 0.05

Fig. 3

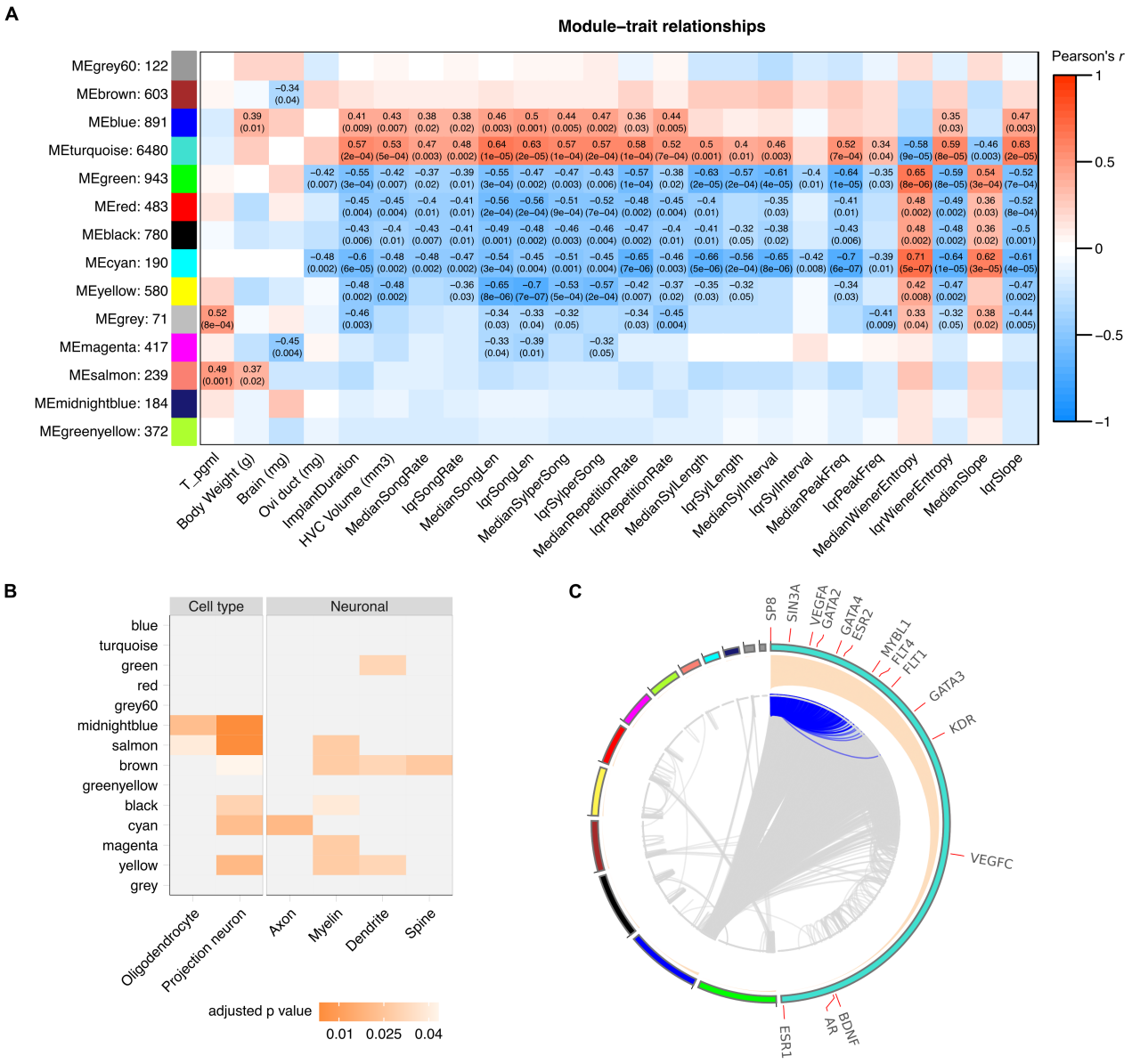
A
Module−trait relationships
Pearson's r
1
0.5
0
−0.5
−1
MEgrey60: 122
MEbrown: 603
MEblue: 891
MEturquoise: 6480
MEgreen: 943
MEred: 483
MEblack: 780
MEcyan: 190
MEyellow: 580
MEgrey: 71
MEmagenta: 417
MEsalmon: 239
MEmidnightblue: 184
MEgreenyellow: 372
T_pgml
Body Weight (g)
Brain (mg)
Ovi duct (mg)
ImplantDuration
HVC Volume (mm3)
MedianSongRate
IqrSongRate
MedianSongLen
IqrSongLen
MedianSylperSong
IqrSylperSong
MedianRepetitionRate
IqrRepetitionRate
MedianSylLength
IqrSylLength
MedianSylInterval
IqrSylInterval
MedianPeakFreq
IqrPeakFreq
MedianWienerEntropy
IqrWienerEntropy
MedianSlope
IqrSlope
B
Cell type
Neuronal
blue
turquoise
green
red
grey60
midnightblue
salmon
brown
greenyellow
black
cyan
magenta
yellow
grey
Oligodendrocyte
Projection neuron
Axon
Myelin
Dendrite
Spine
adjusted p value
0.01
0.025
0.04
C
SP8
SIN3A
VEGFA
GATA2
GATA4
ESR2
MYBL1
FLT4
FLT1
GATA3
KDR
VEGFC
BDNF
AR
ESR1

Fig. 4

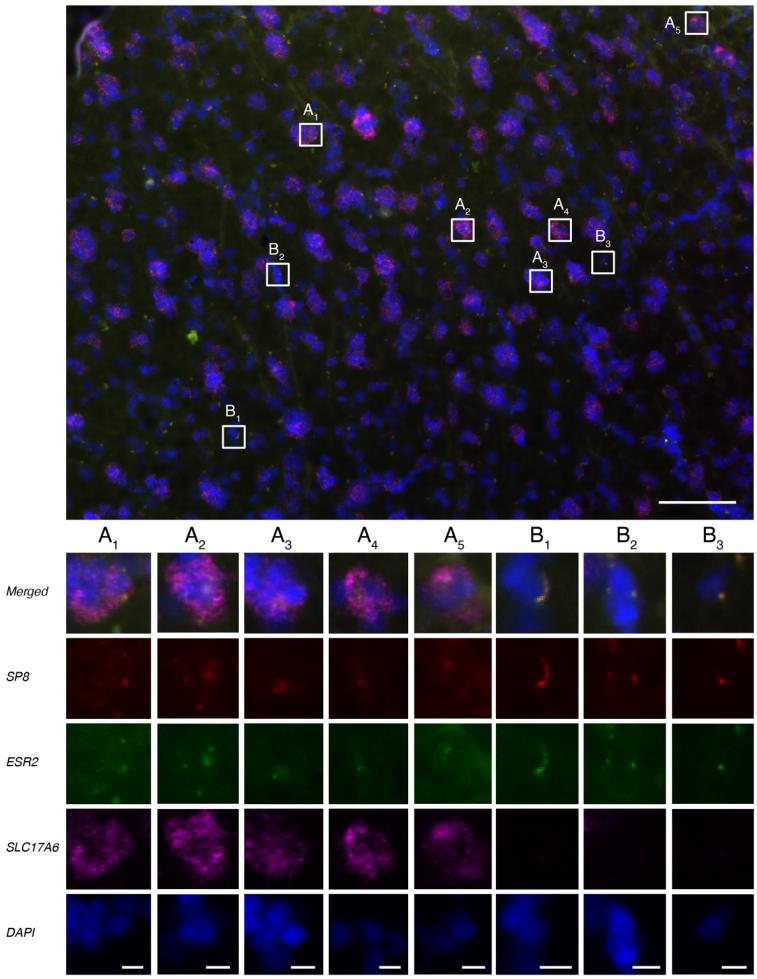

984

985 **Fig. 5**

986

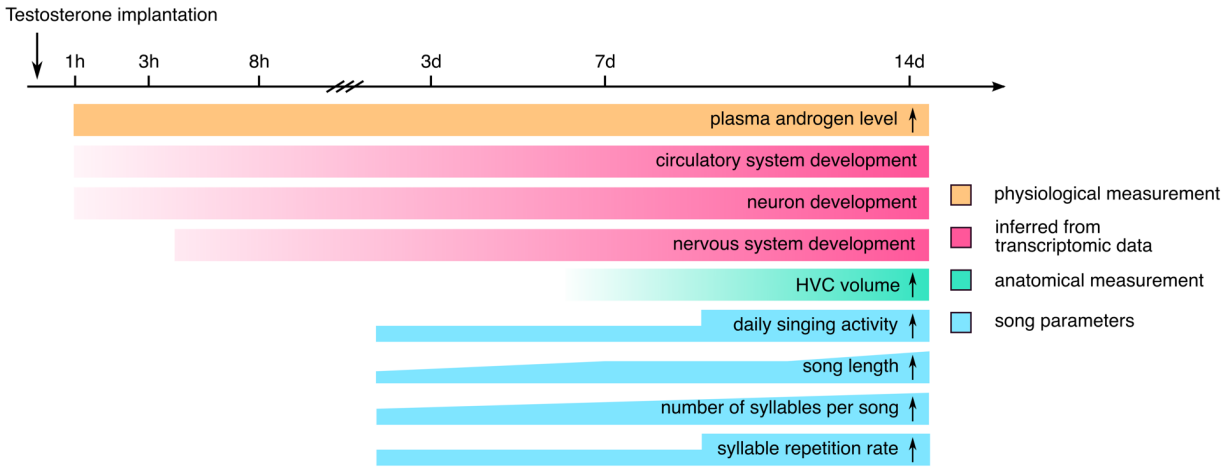
Testosterone implantation
1h
3h
8h
3d
7d
14d
plasma androgen level
circulatory system development
neuron development
nervous system development
HVC volume
daily singing activity
song length
number of syllables per song
syllable repetition rate
physiological measurement
inferred from transcriptomic data
anatomical measurement
song parameters

Fig. 6

References

Alliende, J., Giret, N., Pidoux, L., Del Negro, C., Leblois, A., 2017. Seasonal plasticity of song behavior relies on motor and syntactic variability induced by a basal ganglia-forebrain circuit. Neuroscience 359, 49-68.

Apfelbeck, B., Kiefer, S., Mortega, K.G., Goymann, W., Kipper, S., 2012. Testosterone Affects Song Modulation during Simulated Territorial Intrusions in Male Black Redstarts (Phoenicurus ochruros). PLOS ONE 7, e52009.

Arnold, A.P., Nottebohm, F., Pfaff, D.W., 1976. Hormone concentrating cells in vocal control and other areas of the brain of the zebra finch (Poephila guttata). J Comp Neurol 165, 487-511.

Ashburner, M., Ball, C.A., Blake, J.A., Botstein, D., Butler, H., Cherry, J.M., Davis, A.P., Dolinski, K., Dwight, S.S., Eppig, J.T., Harris, M.A., Hill, D.P., Issel-Tarver, L., Kasarskis, A., Lewis, S., Matese, J.C., Richardson, J.E., Ringwald, M., Rubin, G.M., Sherlock, G., 2000. Gene Ontology: tool for the unification of biology. Nature Genetics 25, 25.

Ball, G.F., Auger, C.J., Bernard, D.J., Charlier, T.D., Sartor, J.J., Riters, L.V., Balthazart, J., 2004. Seasonal plasticity in the song control system: multiple brain sites of steroid hormone action and the importance of variation in song behavior. Ann N Y Acad Sci 1016, 586-610.

Ball, G.F., Balthazart, J., 2002. Neuroendocrine mechanisms regulating reproductive cycles and reproductive behavior in birds, Hormones, brain and behavior. Elsevier, pp. 649-XII.

Bao, R., Onishi, K.G., Tolla, E., Ebling, F.J.P., Lewis, J.E., Anderson, R.L., Barrett, P., Prendergast, B.J., Stevenson, T.J., 2019. Genome sequencing and transcriptome analyses of the Siberian hamster hypothalamus identify mechanisms for seasonal energy balance. Proceedings of the National Academy of Sciences 116, 13116-13121.

Basista, M.J., Elliott, K.C., Wu, W., Hyson, R.L., Bertram, R., Johnson, F., 2014. Independent premotor encoding of the sequence and structure of birdsong in avian cortex. J Neurosci 34, 16821-16834.

Bates, D., Mächler, M., Bolker, B., Walker, S., 2014. Fitting linear mixed-effects models using lme4. arXiv preprint arXiv:1406.5823.

Bell, S.M., Schreiner, C.M., Waclaw, R.R., Campbell, K., Potter, S.S., Scott, W.J., 2003. Sp8 is crucial for limb outgrowth and neuropore closure. Proceedings of the National Academy of Sciences of the United States of America 100, 12195-12200.

Benson, D.A., Karsch-Mizrachi, I., Lipman, D.J., Ostell, J., Wheeler, D.L., 2005. GenBank. Nucleic Acids Research 33, D34-D38.

Bernard, D.J., Bentley, G.E., Balthazart, J., Turek, F.W., Ball, G.F., 1999. Androgen Receptor, Estrogen Receptor α, and Estrogen Receptorβ Show Distinct Patterns of Expression in Forebrain Song Control Nuclei of European Starlings. Endocrinology 140, 4633-4643.

Bindea, G., Mlecnik, B., Hackl, H., Charoentong, P., Tosolini, M., Kirilovsky, A., Fridman, W.-H., Pagès, F., Trajanoski, Z., Galon, J., 2009. ClueGO: a Cytoscape plug-in to decipher functionally grouped gene ontology and pathway annotation networks. Bioinformatics 25, 1091-1093.

1030 Bourdeau, V.r., Deschênes, J., Métivier, R.l., Nagai, Y., Nguyen, D., Bretschneider, N., Gannon, F.,
1031 White, J.H., Mader, S., 2004. Genome-Wide Identification of High-Affinity Estrogen Response
1032 Elements in Human and Mouse. Molecular Endocrinology 18, 1411-1427.

1033 Burkett, Z.D., Day, N.F., Kimball, T.H., Aamodt, C.M., Heston, J.B., Hilliard, A.T., Xiao, X., White,
1034 S.A., 2018. FoxP2 isoforms delineate spatiotemporal transcriptional networks for vocal learning in
1035 the zebra finch. eLife 7, e30649.

1036 Byers, J., Hebets, E., Podos, J., 2010. Female mate choice based upon male motor performance.
1037 Animal Behaviour 79, 771-778.

1038 Cartharius, K., Frech, K., Grote, K., Klocke, B., Haltmeier, M., Klingenhoff, A., Frisch, M.,
1039 Bayerlein, M., Werner, T., 2005. MatInspector and beyond: promoter analysis based on transcription
1040 factor binding sites. Bioinformatics 21, 2933-2942.

1041 Catchpole, C.K., Slater, P.J.B., 2018. Bird Song: Biological Themes and Variations, 2nd ed.

1042 Celec, P., Ostatníková, D., Hodosy, J., 2015. On the effects of testosterone on brain behavioral
1043 functions. Frontiers in Neuroscience 9.

1044 Cheviron, Z.A., Swanson, D.L., 2017. Comparative Transcriptomics of Seasonal Phenotypic
1045 Flexibility in Two North American Songbirds. Integr Comp Biol 57, 1040-1054.

1046 Cohen, C.D., Lindenmeyer, M.T., Eichinger, F., Hahn, A., Seifert, M., Moll, A.G., Schmid, H., Kiss,
1047 E., Grone, E., Grone, H.J., Kretzler, M., Werner, T., Nelson, P.J., 2008. Improved elucidation of
1048 biological processes linked to diabetic nephropathy by single probe-based microarray data analysis.
1049 PLoS One 3, e2937.

1050 Colquitt, B.M., Merullo, D.P., Konopka, G., Roberts, T.F., Brainard, M.S., 2021. Cellular
1051 transcriptomics reveals evolutionary identities of songbird vocal circuits. Science 371, eabd9704.

1052 Consortium, T.G.O., 2017. Expansion of the Gene Ontology knowledgebase and resources. Nucleic
1053 Acids Research 45, D331-D338.

1054 Consortium, T.U., 2015. UniProt: a hub for protein information. Nucleic Acids Research 43, D204-
1055 D212.

1056 Cornez, G., Shevchouk, O.T., Ghorbanpoor, S., Ball, G.F., Cornil, C.A., Balthazart, J., 2020.
1057 Testosterone stimulates perineuronal nets development around parvalbumin cells in the adult canary
1058 brain in parallel with song crystallization. Horm Behav 119, 104643.

1059 de Bournonville, M.P., de Bournonville, C., Vandries, L.M., Nys, G., Fillet, M., Ball, G.F.,
1060 Balthazart, J., Cornil, C.A., 2021. Rapid changes in brain estrogen concentration during male sexual
1061 behavior are site and stimulus specific. Sci Rep 11, 20130.

1062 Dittrich, F., Ramenda, C., Grillitsch, D., Frankl-Vilches, C., Ko, M.C., Hertel, M., Goymann, W.,
1063 Ter Maat, A., Gahr, M., 2014. Regulatory mechanisms of testosterone-stimulated song in the
1064 sensorimotor nucleus HVC of female songbirds. BMC Neurosci 15, 128.

1065 Dopico, X.C., Evangelou, M., Ferreira, R.C., Guo, H., Pekalski, M.L., Smyth, D.J., Cooper, N.,
1066 Burren, O.S., Fulford, A.J., Hennig, B.J., Prentice, A.M., Ziegler, A.G., Bonifacio, E., Wallace, C.,

Todd, J.A., 2015. Widespread seasonal gene expression reveals annual differences in human immunity and physiology. Nat Commun 6, 7000.

Drăgănoiu, T.I., Nagle, L., Kreutzer, M., 2002. Directional female preference for an exaggerated male trait in canary (Serinusanaria) song. Proceedings of the Royal Society of London. Series B: Biological Sciences 269, 2525.

Edgar, R., Domrachev, M., Lash, A., 2002. Gene Expression Omnibus: NCBI gene expression and hybridization array data repository. Nucleic Acids Res 30, 207 - 210.

Faber-Hammond, J., Samanta, M.P., Whitchurch, E.A., Manning, D., Sisneros, J.A., Coffin, A.B., 2015. Saccular Transcriptome Profiles of the Seasonal Breeding Plainfin Midshipman Fish (Porichthys notatus), a Teleost with Divergent Sexual Phenotypes. PLoS One 10, e0142814.

Flicek, P., Amode, M.R., Barrell, D., Beal, K., Billis, K., Brent, S., Carvalho-Silva, D., Clapham, P., Coates, G., Fitzgerald, S., Gil, L., Girón, C.G., Gordon, L., Hourlier, T., Hunt, S., Johnson, N., Juettemann, T., Kähäri, A.K., Keenan, S., Kulesha, E., Martin, F.J., Maurel, T., McLaren, W.M., Murphy, D.N., Nag, R., Overduin, B., Pignatelli, M., Pritchard, B., Pritchard, E., Riat, H.S., Ruffier, M., Sheppard, D., Taylor, K., Thormann, A., Trevanion, S.J., Vullo, A., Wilder, S.P., Wilson, M., Zadissa, A., Aken, B.L., Birney, E., Cunningham, F., Harrow, J., Herrero, J., Hubbard, T.J.P., Kinsella, R., Muffato, M., Parker, A., Spudich, G., Yates, A., Zerbino, D.R., Searle, S.M.J., 2014. Ensembl 2014. Nucleic Acids Research 42, D749-D755.

Forlano, P.M., Sisneros, J.A., Rohmann, K.N., Bass, A.H., 2015. Neuroendocrine control of seasonal plasticity in the auditory and vocal systems of fish. Front Neuroendocrinol 37, 129-145.

Frankl-Vilches, C., Gahr, M., 2017. Androgen and estrogen sensitivity of bird song: a comparative view on gene regulatory levels. Journal of Comparative Physiology A.

Frankl-Vilches, C., Kuhl, H., Werber, M., Klages, S., Kerick, M., Bakker, A., de Oliveira, E.H., Reusch, C., Capuano, F., Vowinckel, J., Leitner, S., Ralser, M., Timmermann, B., Gahr, M., 2015. Using the canary genome to decipher the evolution of hormone-sensitive gene regulation in seasonal singing birds. Genome Biol 16, 19.

Fuentes, N., Silveyra, P., 2019. Estrogen receptor signaling mechanisms. Adv Protein Chem Struct Biol 116, 135-170.

Fusani, L., Metzdorf, R., Hutchison, J., Gahr, M., 2003. Aromatase inhibition affects testosterone-induced masculinization of song and the neural song system in female canaries. J Neurobiol 54, 370 - 379.

Gaborieau, E., Hurtado-Chong, A., Fernández, M., Azim, K., Raineteau, O., 2018. A dual role for the transcription factor Sp8 in postnatal neurogenesis. Scientific Reports 8, 14560.

Gahr, M., 1990a. Delineation of a brain nucleus: comparisons of cytochemical, hodological, and cytoarchitectural views of the song control nucleus HVc of the adult canary. J Comp Neurol 294, 30-36.

Gahr, M., 1990b. Localization of androgen receptors and estrogen receptors in the same cells of the songbird brain. Proc Natl Acad Sci U S A 87, 9445 - 9448.

1105 Gahr, M., 2001. Distribution of sex steroid hormone receptors in the avian brain: Functional
1106 implications for neural sex differences and sexual behaviors. Microscopy Research and Technique
1107 55, 1-11.

1108 Gahr, M., 2004. Hormone-dependent neural plasticity in the juvenile and adult song system: what
1109 makes a successful male? Ann N Y Acad Sci 1016, 684-703.

1110 Gahr, M., 2014. How Hormone-Sensitive Are Bird Songs And What Are The Underlying
1111 Mechanisms? Acta Acustica United with Acustica 100, 705-718.

1112 Gahr, M., 2020. Seasonal hormone fluctuations and song structure of birds. Coding strategies in
1113 vertebrate acoustic communication, 163-201.

1114 Gahr, M., Garcia-Segura, L.M., 1996. Testosterone-dependent increase of gap-junctions in HVC
1115 neurons of adult female canaries. Brain Research 712, 69-73.

1116 Gahr, M., Metzdorf, R., 1997. Distribution and dynamics in the expression of androgen and estrogen
1117 receptors in vocal control systems of songbirds. Brain Res Bull 44, 509 - 517.

1118 Gahr, M., Wild, J.M., 1997. Localization of androgen receptor mRNA-containing cells in avian
1119 respiratory-vocal nuclei: an in situ hybridization study. J Neurobiol 33, 865-876.

1120 Gardner, M., 1978. White and brown music, fractal curves and one-over-f fluctuations. Scientific
1121 American 238, 16-33.

1122 Gautier, L., Cope, L., Bolstad, B.M., Irizarry, R.A., 2004. affy—analysis of Affymetrix GeneChip
1123 data at the probe level. Bioinformatics 20, 307-315.

1124 Gelman, A., Hill, J., 2006. Data analysis using regression and multilevel/hierarchical models.
1125 Cambridge university press.

1126 Gelman, A., Su, Y.-S., 2018. arm: Data Analysis Using Regression and Multilevel/Hierarchical
1127 Models, 1.10-1 ed, pp. R package version 1.10-11.

1128 Genomatix. Precigen Bioinformatics Germany GmbH (PBG), http://www.genomatix.de.

1129 Gisiger, T., 2001. Scale invariance in biology: coincidence or footprint of a universal mechanism?
1130 Biological Reviews 76, 161-209.

1131 Godsave, S.F., Lohmann, R., Vloet, R.P., Gahr, M., 2002. Androgen receptors in the embryonic
1132 zebra finch hindbrain suggest a function for maternal androgens in perihatching survival. J Comp
1133 Neurol 453, 57-70.

1134 Goldin, M.A., Alonso, L.M., Alliende, J.A., Goller, F., Mindlin, G.B., 2013. Temperature induced
1135 syllable breaking unveils nonlinearly interacting timescales in birdsong motor pathway. PLoS One 8,
1136 e67814.

1137 Goldman, S., Nottebohm, F., 1983. Neuronal production, migration, and differentiation in a vocal
1138 control nucleus in the adult female canary brain. Proc Natl Acad Sci U S A 80, 2390.

1139 Goymann, W., Möstl, E., Gwinner, E., 2002. Non-invasive methods to measure androgen
1140 metabolites in excrements of European stonechats, Saxicola torquata rubicola. General and
1141 Comparative Endocrinology 129, 80-87.

1142 Guh, Y.-J., Tamai, T.K., Yoshimura, T., 2019. The underlying mechanisms of vertebrate seasonal
1143 reproduction. Proceedings of the Japan Academy, Series B 95, 343-357.

1144 Guillemette, C., 2003. Pharmacogenomics of human UDP-glucuronosyltransferase enzymes. The
1145 Pharmacogenomics Journal 3, 136.

1146 Hahnloser, R.H.R., Kozhevnikov, A.A., Fee, M.S., 2002. An ultra-sparse code underliesthe
1147 generation of neural sequences in a songbird. Nature 419, 65-70.

1148 Hartley, R.S., Chinn, M.S., Ullrich, N.F.E., 1997. Left Syringeal Dominance in Testosterone-Treated
1149 Female Canaries. Neurobiology of Learning and Memory 67, 248-253.

1150 Hartog, T., Dittrich, F., Pieneman, A., Jansen, R., Frankl-Vilches, C., Lessmann, V., 2009. Brain-
1151 derived neurotrophic factor signaling in the HVC is required for testosterone-induced song of female
1152 canaries. J Neurosci 29, 15511 - 15519.

1153 Hausberger, M., Henry, L., Richard, M.A., 1995. Testosterone-induced Singing in Female European
1154 Starlings (Sturnus vulgaris). Ethology 99, 193-208.

1155 Herrick, E.H., Harris, J.O., 1957. Singing Female Canaries. Science 125, 1299-1300.

1156 Huang, D.W., Sherman, B.T., Lempicki, R.A., 2008. Systematic and integrative analysis of large
1157 gene lists using DAVID bioinformatics resources. Nature Protocols 4, 44-57.

1158 Huang, D.W., Sherman, B.T., Lempicki, R.A., 2009. Bioinformatics enrichment tools: paths toward
1159 the comprehensive functional analysis of large gene lists. Nucleic Acids Research 37, 1-13.

1160 Jarvis, E.D., Nottebohm, F., 1997. Motor-driven gene expression. Proceedings of the National
1161 Academy of Sciences 94, 4097-4102.

1162 Jennings, K.J., de Lecea, L., 2020. Neural and Hormonal Control of Sexual Behavior. Endocrinology
1163 161.

1164 Jia, Y., Castellanos, J., Wang, C., Sinha-Hikim, I., Lue, Y., Swerdloff, R.S., Sinha-Hikim, A.P.,
1165 2009. Mitogen-activated protein kinase signaling in male germ cell apoptosis in the rat. Biol Reprod
1166 80, 771-780.

1167 Johnson, F., Bottjer, S.W., 1993. Hormone-induced changes in identified cell populations of the
1168 higher vocal center in male canaries. Journal of Neurobiology 24, 400-418.

1169 Johnson, F., Bottjer, S.W., 1995. Differential estrogen accumulation among populations of projection
1170 neurons in the higher vocal center of male canaries. Journal of Neurobiology 26, 87-108.

1171 Kim, D.-H., Lilliehook, C., Roides, B., Chen, Z., Chang, M., Mobashery, S., Goldman, S.A., 2008.
1172 Testosterone-Induced Matrix Metalloproteinase Activation Is a Checkpoint for Neuronal Addition to
1173 the Adult Songbird Brain. The Journal of Neuroscience 28, 208.

Ko, M.-C., Frankl-Vilches, C., Bakker, A., Gahr, M., 2021. The Gene Expression Profile of the Song Control Nucleus HVC Shows Sex Specificity, Hormone Responsiveness, and Species Specificity Among Songbirds. Frontiers in Neuroscience 15.

Ko, M.-C., Van Meir, V., Vellema, M., Gahr, M., 2020. Characteristics of song, brain-anatomy and blood androgen levels in spontaneously singing female canaries. Hormones and Behavior 117, 104614.

Korner-Nievergelt, F., Roth, T., Von Felten, S., Guélat, J., Almasi, B., Korner-Nievergelt, P., 2015. Bayesian data analysis in ecology using linear models with R, BUGS, and Stan. Academic Press.

Langfelder, P., Horvath, S., 2008. WGCNA: an R package for weighted correlation network analysis. BMC Bioinformatics 9, 1-13.

Langfelder, P., Horvath, S., 2012. Fast R Functions for Robust Correlations and Hierarchical Clustering. Journal of statistical software 46, i11.

Larson, T.A., Lent, K.L., Bammler, T.K., MacDonald, J.W., Wood, W.E., Caras, M.L., Thatra, N.M., Budzillo, A., Perkel, D.J., Brenowitz, E.A., 2015. Network analysis of microRNA and mRNA seasonal dynamics in a highly plastic sensorimotor neural circuit. BMC genomics 16, 905.

Leitner, S., Voigt, C., Garcia-Segura, L., Van't Hof, T., Gahr, M., 2001. Seasonal activation and inactivation of song motor memories in wild canaries is not reflected in neuroanatomical changes of forebrain song areas. Horm Behav 40, 160 - 168.

Limame, R., de Beeck, K.O., Lardon, F., Wever, O.D., Pauwels, P., 2014. Krüppel-like factors in cancer progression: three fingers on the steering wheel. Oncotarget 5, 29-48.

Limbourg, F.P., Takeshita, K., Radtke, F., Bronson, R.T., Chin, M.T., Liao, J.K., 2005. Essential role of endothelial Notch1 in angiogenesis. Circulation 111, 1826-1832.

Long, M.A., Fee, M.S., 2008. Using temperature to analyse temporal dynamics in the songbird motor pathway. Nature 456, 189-194.

Louissaint, A., Rao, S., Leventhal, C., Goldman, S.A., 2002. Coordinated Interaction of Neurogenesis and Angiogenesis in the Adult Songbird Brain. Neuron 34, 945-960.

Lovell, P.V., Carleton, J.B., Mello, C.V., 2013. Genomics analysis of potassium channel genes in songbirds reveals molecular specializations of brain circuits for the maintenance and production of learned vocalizations. BMC genomics 14, 470.

Madison, F.N., Rouse, M.L., Jr., Balthazart, J., Ball, G.F., 2015. Reversing song behavior phenotype: Testosterone driven induction of singing and measures of song quality in adult male and female canaries (Serinus canaria). Gen Comp Endocrinol 215, 61-75.

Marynick, S.P., Havens, W.W., 2nd, Ebert, M.H., Loriaux, D.L., 1976. Studies on the transfer of steroid hormones across the blood-cerebrospinal fluid barrier in the Rhesus Monkey. Endocrinology 99, 400-405.

Metzdorf, R., Gahr, M., Fusani, L., 1999. Distribution of aromatase, estrogen receptor, and androgen receptor mRNA in the forebrain of songbirds and nonsongbirds. J Comp Neurol 407, 115-129.

1211 Michels, G., Hoppe, U.C., 2008. Rapid actions of androgens. Front Neuroendocrinol 29, 182-198.

1212 Migaud, M., Butrille, L., Batailler, M., 2015. Seasonal regulation of structural plasticity and
1213 neurogenesis in the adult mammalian brain: focus on the sheep hypothalamus. Front
1214 Neuroendocrinol 37, 146-157.

1215 Miller, J.A., Cai, C., Langfelder, P., Geschwind, D.H., Kurian, S.M., Salomon, D.R., Horvath, S.,
1216 2011. Strategies for aggregating gene expression data: The collapseRows R function. BMC
1217 Bioinformatics 12, 322.

1218 Morey, J.S., Neely, M.G., Lunardi, D., Anderson, P.E., Schwacke, L.H., Campbell, M., Van Dolah,
1219 F.M., 2016. RNA-Seq analysis of seasonal and individual variation in blood transcriptomes of
1220 healthy managed bottlenose dolphins. BMC genomics 17, 720.

1221 Nottebohm, F., 1980. Testosterone triggers growth of brain vocal control nuclei in adult female
1222 canaries. Brain Res 189, 429-436.

1223 Nottebohm, F., 1981. A brain for all seasons: cyclical anatomical changes in song control nuclei of
1224 the canary brain. Science 214, 1368.

1225 Nottebohm, F., Nottebohm, M.E., Crane, L., 1986. Developmental and seasonal changes in canary
1226 song and their relation to changes in the anatomy of song-control nuclei. Behavioral and neural
1227 biology 46, 445-471.

1228 Nottebohm, F., Stokes, T.M., Leonard, C.M., 1976. Central control of song in the canary, Serinus
1229 canarius. The Journal of Comparative Neurology 165, 457-486.

1230 Ouzzine, M., Gulberti, S., Ramalanjaona, N., Magdalou, J., Fournel-Gigleux, S., 2014. The UDP-
1231 glucuronosyltransferases of the blood-brain barrier: their role in drug metabolism and detoxication.
1232 Frontiers in Cellular Neuroscience 8.

1233 Pesch, A., Güttinger, H.-R., 1985. Der Gesang des weiblichen Kanarienvogels. J Ornithol 126, 108-
1234 110.

1235 Peterson, M.P., Rosvall, K.A., Choi, J.H., Ziegenfus, C., Tang, H., Colbourne, J.K., Ketterson, E.D.,
1236 2013. Testosterone affects neural gene expression differently in male and female juncos: a role for
1237 hormones in mediating sexual dimorphism and conflict. PLoS One 8, e61784.

1238 Pi, M., Parrill, A.L., Quarles, L.D., 2010. GPRC6A Mediates the Non-genomic Effects of Steroids.
1239 Journal of Biological Chemistry 285, 39953-39964.

1240 Pihlajamaa, P., Sahu, B., Jänne, O.A., 2015. Determinants of Receptor- and Tissue-Specific Actions
1241 in Androgen Signaling. Endocrine Reviews 36, 357-384.

1242 Pihlajamaa, P., Sahu, B., Lyly, L., Aittomäki, V., Hautaniemi, S., Jänne, O.A., 2014. Tissue-specific
1243 pioneer factors associate with androgen receptor cistromes and transcription programs. The EMBO
1244 Journal 33, 312-326.

1245 Quandt, K., Frech, K., Karas, H., Wingender, E., Werner, T., 1995. Matlnd and Matlnspector: new
1246 fast and versatile tools for detection of consensus matches in nucleotide sequence data. Nucleic
1247 Acids Research 23, 4878-4884.

1248 Quispe, R., Trappschuh, M., Gahr, M., Goymann, W., 2015. Towards more physiological
1249 manipulations of hormones in field studies: comparing the release dynamics of three kinds of
1250 testosterone implants, silastic tubing, time-release pellets and beeswax. Gen Comp Endocrinol 212,
1251 100-105.

1252 Rasika, S., Alvarez-Buylla, A., Nottebohm, F., 1999. BDNF mediates the effects of testosterone on
1253 the survival of new neurons in an adult brain. Neuron 22, 53-62.

1254 Rasika, S., Nottebohm, F., Alvarez-Buylla, A., 1994. Testosterone increases the recruitment and/or
1255 survival of new high vocal center neurons in adult female canaries. Proc Natl Acad Sci U S A 91,
1256 7854-7858.

1257 Reményi, A., Schöler, H.R., Wilmanns, M., 2004. Combinatorial control of gene expression. Nature
1258 Structural &Amp; Molecular Biology 11, 812.

1259 Riebel, K., Odom, K.J., Langmore, N.E., Hall, M.L., 2019. New insights from female bird song:
1260 towards an integrated approach to studying male and female communication roles. Biology Letters
1261 15, 20190059.

1262 Riters, L.V., Eens, M., Pinxten, R., Duffy, D.L., Balthazart, J., Ball, G.F., 2000. Seasonal changes in
1263 courtship song and the medial preoptic area in male European starlings (Sturnus vulgaris). Horm
1264 Behav 38, 250-261.

1265 Rueden, C.T., Schindelin, J., Hiner, M.C., DeZonia, B.E., Walter, A.E., Arena, E.T., Eliceiri, K.W.,
1266 2017. ImageJ2: ImageJ for the next generation of scientific image data. BMC Bioinformatics 18,
1267 529.

1268 Safe, S., Kim, K., 2008. Non-classical genomic estrogen receptor (ER)/specificity protein and
1269 ER/activating protein-1 signaling pathways. Journal of Molecular Endocrinology 41, 263-275.

1270 Sartor, J.J., Balthazart, J., Ball, G.F., 2005. Coordinated and dissociated effects of testosterone on
1271 singing behavior and song control nuclei in canaries (Serinus canaria). Horm Behav 47, 467-476.

1272 Schindelin, J., Arganda-Carreras, I., Frise, E., Kaynig, V., Longair, M., Pietzsch, T., Preibisch, S.,
1273 Rueden, C., Saalfeld, S., Schmid, B., Tinevez, J.-Y., White, D.J., Hartenstein, V., Eliceiri, K.,
1274 Tomancak, P., Cardona, A., 2012. Fiji: an open-source platform for biological-image analysis.
1275 Nature Methods 9, 676.

1276 Schlinger, B., Scanes, C., Randhawa, M., Callard, G., 1984. Distribution of aromatase activity in
1277 quail brain (Cc japonica): effects of photoperiod and castration. Journal of Steroid Biochemistry 20,
1278 1571.

1279 Schwartz, C., Andrews, M.T., 2013. Circannual transitions in gene expression: lessons from seasonal
1280 adaptations. Curr Top Dev Biol 105, 247-273.

1281 Schwartz, C., Hampton, M., Andrews, M.T., 2013. Seasonal and regional differences in gene
1282 expression in the brain of a hibernating mammal. PloS one 8, e58427-e58427.

1283 Shannon, P., Markiel, A., Ozier, O., Baliga, N.S., Wang, J.T., Ramage, D., Amin, N., Schwikowski,
1284 B., Ideker, T., 2003. Cytoscape: a software environment for integrated models of biomolecular
1285 interaction networks. Genome Res 13, 2498-2504.

1286 Sharma, A., Das, S., Kumar, V., 2019. Transcriptome-wide changes in testes reveal molecular
1287 differences in photoperiod-induced seasonal reproductive life-history states in migratory songbirds.
1288 Mol Reprod Dev 86, 956-963.

1289 Sharp, P.J., Armstrong, D.G., Moss, R., 1986. Changes in aromatase activity in the neuroendocrine
1290 tissues of red grouse (Lagopus lagopus scoticus) in relation to the development of long-day
1291 refractoriness. J Endocrinol 108, 129-135.

1292 Shoemaker, H.H., 1939. Effect of Testosterone Propionate on Behavior of the Female Canary.
1293 Proceedings of the Society for Experimental Biology and Medicine 41, 299-302.

1294 Snijders, L., van Oers, K., Naguib, M., 2017. Sex-specific responses to territorial intrusions in a
1295 communication network: Evidence from radio-tagged great tits. Ecol Evol 7, 918-927.

1296 Sui, S.J.H., Mortimer, J.R., Arenillas, D.J., Brumm, J., Walsh, C.J., Kennedy, B.P., Wasserman,
1297 W.W., 2005. oPOSSUM: identification of over-represented transcription factor binding sites in co-
1298 expressed genes. Nucleic Acids Research 33, 3154-3164.

1299 Szklarczyk, D., Franceschini, A., Wyder, S., Forslund, K., Heller, D., Huerta-Cepas, J., Simonovic,
1300 M., Roth, A., Santos, A., Tsafou, K.P., Kuhn, M., Bork, P., Jensen, L.J., von Mering, C., 2015.
1301 STRING v10: protein–protein interaction networks, integrated over the tree of life. Nucleic Acids
1302 Research 43, D447-D452.

1303 Takayama, K., Kaneshiro, K., Tsutsumi, S., Horie-Inoue, K., Ikeda, K., Urano, T., Ijichi, N., Ouchi,
1304 Y., Shirahige, K., Aburatani, H., Inoue, S., 2007. Identification of novel androgen response genes in
1305 prostate cancer cells by coupling chromatin immunoprecipitation and genomic microarray analysis.
1306 Oncogene 26, 4453.

1307 Tchernichovski, O., Nottebohm, F., Ho, C.E., Pesaran, B., Mitra, P.P., 2000. A procedure for an
1308 automated measurement of song similarity. Anim Behav 59, 1167-1176.

1309 Team, R.C., 2020. R: A language and environment for statistical computing. R Foundation for
1310 Statistical Computing [Internet]. Vienna, Austria.

1311 Thompson, C., Meitzen, J., Replogle, K., Drnevich, J., Lent, K., Wissman, A., 2012. Seasonal
1312 changes in patterns of gene expression in avian song control brain regions. PLoS One 7, e35119.

1313 Tian, F., Liu, S., Shi, J., Qi, H., Zhao, K., Xie, B., 2019. Transcriptomic profiling reveals molecular
1314 regulation of seasonal reproduction in Tibetan highland fish, Gymnocypris przewalskii. BMC
1315 genomics 20, 2-2.

1316 Tusher, V.G., Tibshirani, R., Chu, G., 2001. Significance analysis of microarrays applied to the
1317 ionizing radiation response. Proc Natl Acad Sci U S A 98, 5116-5121.

1318 Vallet, E., Kreutzer, M., Gahr, M., 1996. Testosterone Induces Sexual Release Quality in the Song of
1319 Female Canaries. Ethology 102, 617-628.

1320 Vellema, M., Diales Rocha, M., Bascones, S., Zsebők, S., Dreier, J., Leitner, S., Van der Linden, A.,
1321 Brewer, J., Gahr, M., 2019. Accelerated redevelopment of vocal skills is preceded by lasting
1322 reorganization of the song motor circuitry. eLife 8, e43194.

Voigt, C., Leitner, S., 2008. Seasonality in song behaviour revisited: Seasonal and annual variants and invariants in the song of the domesticated canary (Serinus canaria). Hormones and Behavior 54, 373-378.

Voss, R.F., Clarke, J., 1975. '1/f noise' in music and speech. Nature 258, 317-318.

Waclaw, R.R., Allen, Z.J., Bell, S.M., Erdélyi, F., Szabó, G., Potter, S.S., Campbell, K., 2006. The Zinc Finger Transcription Factor Sp8 Regulates the Generation and Diversity of Olfactory Bulb Interneurons. Neuron 49, 503-516.

Wang, F., Flanagan, J., Su, N., Wang, L.-C., Bui, S., Nielson, A., Wu, X., Vo, H.-T., Ma, X.-J., Luo, Y., 2012. RNAscope: A Novel in Situ RNA Analysis Platform for Formalin-Fixed, Paraffin-Embedded Tissues. The Journal of Molecular Diagnostics 14, 22-29.

Warren, W., Clayton, D., Ellegren, H., Arnold, A., Hillier, L., Kunstner, A., 2010. The genome of a songbird. Nature 464, 757-762.

Watts, H.E., 2020. Seasonal regulation of behaviour: what role do hormone receptors play? Proceedings of the Royal Society B: Biological Sciences 287, 20200722.

Weems, P.W., Goodman, R.L., Lehman, M.N., 2015. Neural mechanisms controlling seasonal reproduction: Principles derived from the sheep model and its comparison with hamsters. Frontiers in Neuroendocrinology 37, 43-51.

Wickham, H., 2009. ggplot2 - Elegant Graphics for Data Analysis, in: Gentleman, R., Hornik, Kurt, Parmigiani, Giovanni (Ed.), Use R! Springer-Verlag, New York, pp. VIII, 213.

Wickler, W., Seibt, U., 1980. Vocal Dueting and the Pair Bond II. Unisono dueting of the African forest weaver, Symplectes bicolor. Zeitschrift für Tierpsychologie 52, 217-226.

Wild, J.M., 2004. Functional Neuroanatomy of the Sensorimotor Control of Singing. Annals of the New York Academy of Sciences 1016, 438-462.

Wilson, S., Qi, J., Filipp, F.V., 2016. Refinement of the androgen response element based on ChIP-Seq in androgen-insensitive and androgen-responsive prostate cancer cell lines. Scientific Reports 6, 32611.

Wingfield, J.C., Smith, J.P., Farner, D.S., 1982. Endocrine Responses of White-Crowned Sparrows to Environmental Stress. The Condor 84, 399-409.

Yates, A., Akanni, W., Amode, M.R., Barrell, D., Billis, K., Carvalho-Silva, D., Cummins, C., Clapham, P., Fitzgerald, S., Gil, L., Girón, C.G., Gordon, L., Hourlier, T., Hunt, S.E., Janacek, S.H., Johnson, N., Juettemann, T., Keenan, S., Lavidas, I., Martin, F.J., Maurel, T., McLaren, W., Murphy, D.N., Nag, R., Nuhn, M., Parker, A., Patricio, M., Pignatelli, M., Rahtz, M., Riat, H.S., Sheppard, D., Taylor, K., Thormann, A., Vullo, A., Wilder, S.P., Zadissa, A., Birney, E., Harrow, J., Muffato, M., Perry, E., Ruffier, M., Spudich, G., Trevanion, S.J., Cunningham, F., Aken, B.L., Zerbino, D.R., Flicek, P., 2016. Ensembl 2016. Nucleic Acids Research 44, D710-D716.

Yu, A.C., Margoliash, D., 1996. Temporal hierarchical control of singing in birds. Science 273, 1871-1875.

Zembrzycki, A., Griesel, G., Stoykova, A., Mansouri, A., 2007. Genetic interplay between the transcription factors Sp8 and Emx2 in the patterning of the forebrain. Neural Development 2, 8.

Zhang, W., Guo, Y., Li, J., Huang, L., Kazitsa, E.G., Wu, H., 2016. Transcriptome analysis reveals the genetic basis underlying the seasonal development of keratinized nuptial spines in Leptobrachium boringii. BMC genomics 17, 978.

Zhao, W., Yuan, T., Fu, Y., Niu, D., Chen, W., Chen, L., Lu, L., 2021. Seasonal differences in the transcriptome profile of the Zhedong white goose (Anser cygnoides) pituitary gland. Poult Sci 100, 1154-1166.

Zornik, E., Kelley, D.B., 2011. A neuroendocrine basis for the hierarchical control of frog courtship vocalizations. Front Neuroendocrinol 32, 353-366.

1371 **Tables**

1372 **Table 1. Experimental groups and sample sizes.**

Group	Sex	Singing	Tissue sampled	Sample size (n)			
				HVC volume	Microarray	Brain weight	Blood plasma testosterone, body weight, and oviduct weight
CON	Female	No	HVC	6	5	6	6
T1h	Female	No	HVC	6	6	6	6
T3h	Female	No	HVC	5	5	5	5
T8h	Female	No	HVC	9	5	8	9
T3d	Female	No	HVC	6	6	9	9
T7d	Female	Yes	HVC	6	6	6	6
T14d	Female	Yes	HVC	6	6	6	6

1373 CON: control birds treated with empty implants; HVC: used as a proper name. Testosterone treatments:

1374 1 hour (h) [T1h], 3 h [T3h], 8 h [T8h], 3 days (d) [T3d], 7 d [T7d], and 14 d [T14d].

1375

Supplementary Figures and Legends

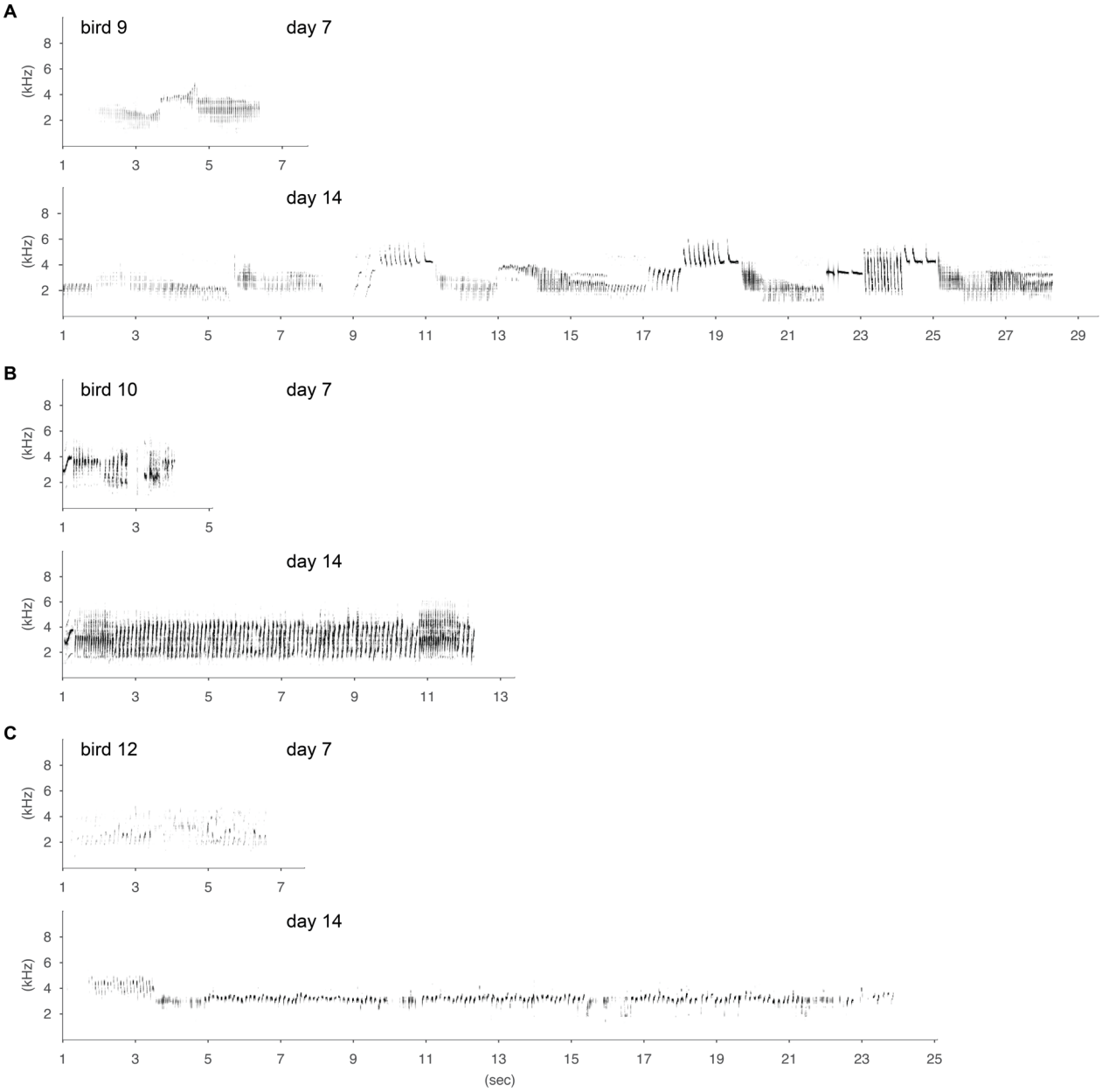

Supplementary Fig. 1**. Representative song spectrograms of the song development of three T14d birds.** Note that the song length, syllable repetitions, and amplitude (the intensity of the spectrogram) of the three birds increased over time. Bird 9 developed the most male-typical song patterns.

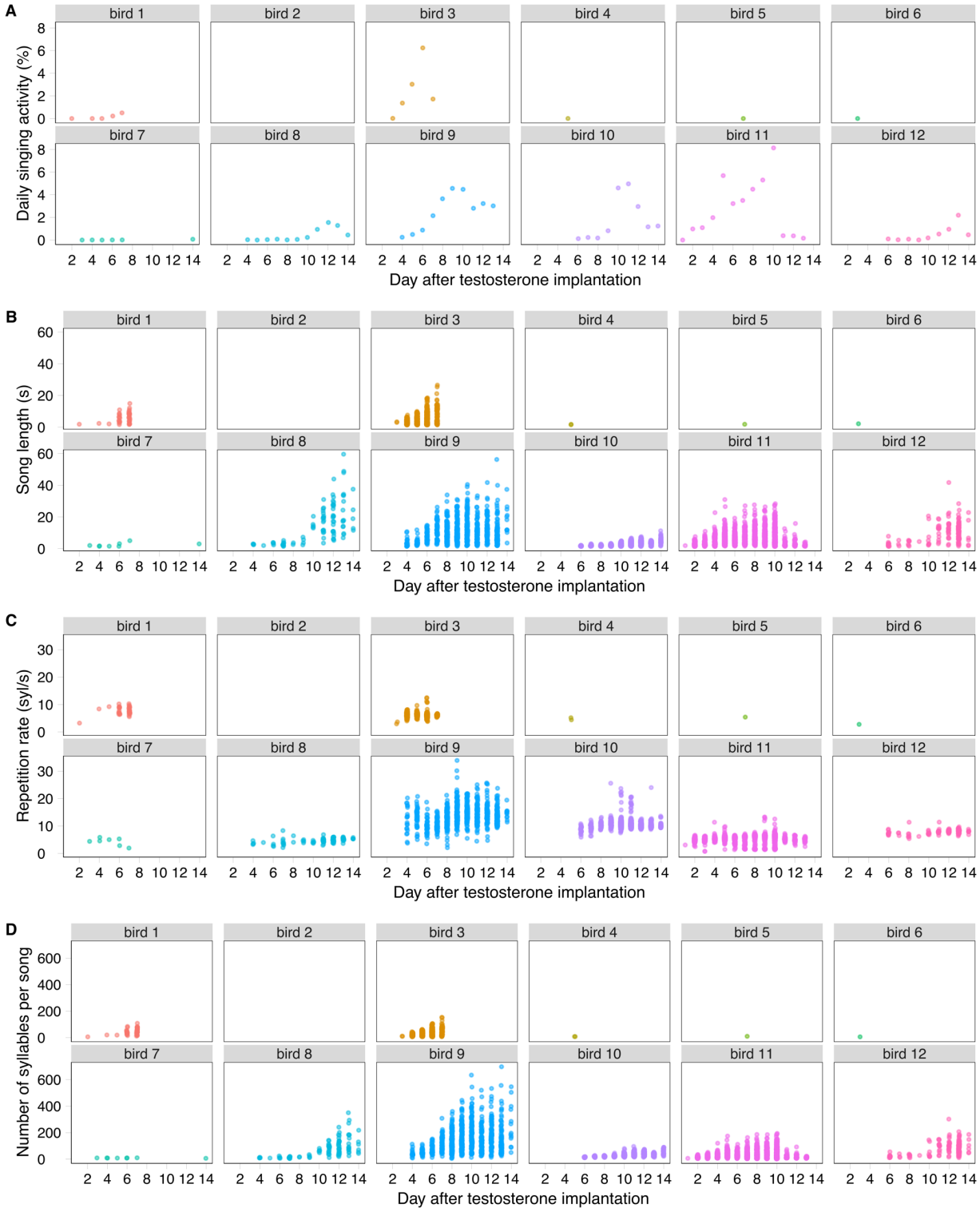

Supplementary Fig. 2. Inter- and intra-individual variability of daily singing activity (A), song length (B), syllable repetition rate (C) and number of syllables per song (D) during song development. Each dot represents a measurement of a day in A and represents a song in B-D. Bird 1 to 6 belong to T7d and bird 7 to 12 belongs to T14d.

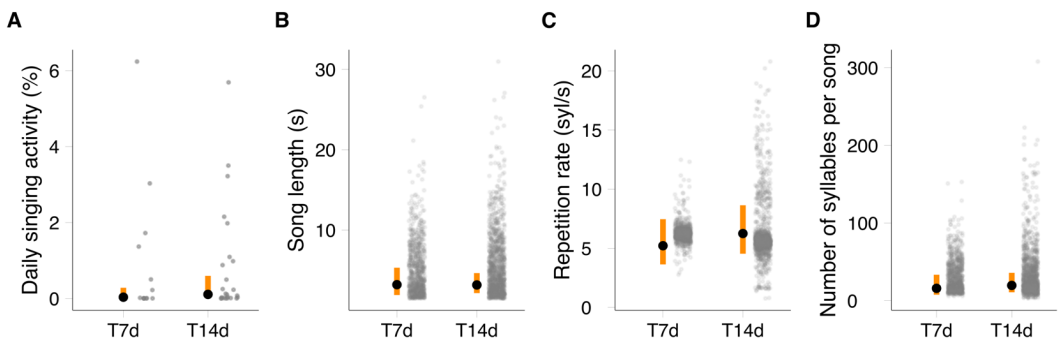

Supplementary Fig. 3. Song parameters quantified during the first seven days after testosterone implantation of female canaries. A, Daily singing activity as measured by the percentage of time spent singing within nine hours per day; **B**, song length in seconds (s); **C**, syllable repetition rate in syllables per second (sys/s); **D**, number of syllables in a song. Each gray dot represents the value per day of a bird in the T7d and T14d groups from day 1 to day 7 after testosterone implantation. The black dots indicate the predicted estimates of the linear mixed-effects models, and the vertical orange bars indicate the 95% credibility intervals (CrI) of the predicted estimates. There are no statistical differences between birds in these two groups, as can be seen from the overlapping 95% CRIs. See also Supplemental Table 2 and supplemental Table 3 for the linear mixed-effect model estimates and posterior probability.

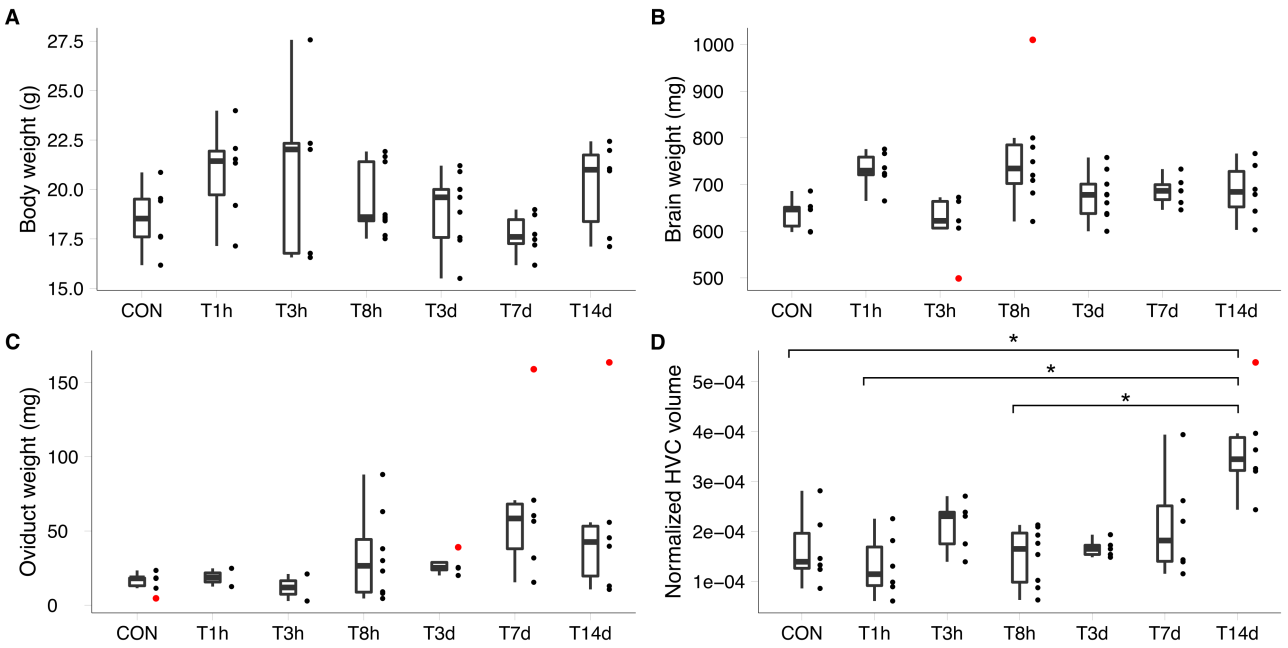

Supplementary Fig. 4. Physiological measurements of testosterone-implanted female canaries. A, no significant differences between control and testosterone-implanted groups in body weight (Kruskal-Wallis rank sum test, $\chi^2 = 7.66$, df = 6, P-value = 0.26). **B**, no significant differences between control and testosterone-implanted groups in brain weight (Kruskal-Wallis rank sum test, $\chi^2 = 17.99$, df = 6, P-value = 0.0063. Dunn's post hoc test, P-value adjusted by Holm' method detected no significantly different pairs). **C**, no significant differences between control and testosterone-implanted groups in oviduct weight (Kruskal-Wallis rank sum test, $\chi^2 = 10.07$, df = 6, P-value = 0.12). **D**, normalized HVC volume (against brain weight) of T14d were significantly different from that of control (CON), T1h, and T8h groups (Kruskal-Wallis rank sum test, $\chi^2 = 17.86$, df = 6, P-value = 0.0065; Holm-adjusted P-value: CON vs. T14d 0.049; T1h vs. T14d 0.0056; T8h vs. T14d 0.016). The boxes indicate the 25th/50th/75th percentiles (bottom/middle/top bar), and the extent of the whiskers indicates the most extreme values that are within 1.5 times of the inter-quartile range (IQR) of the hinge. Outliers are labeled in red. *: Holm-adjusted P-value <0.05 (Kruskal-Wallis rank sum test followed by Dunn's post hoc test using the "Holm" method).

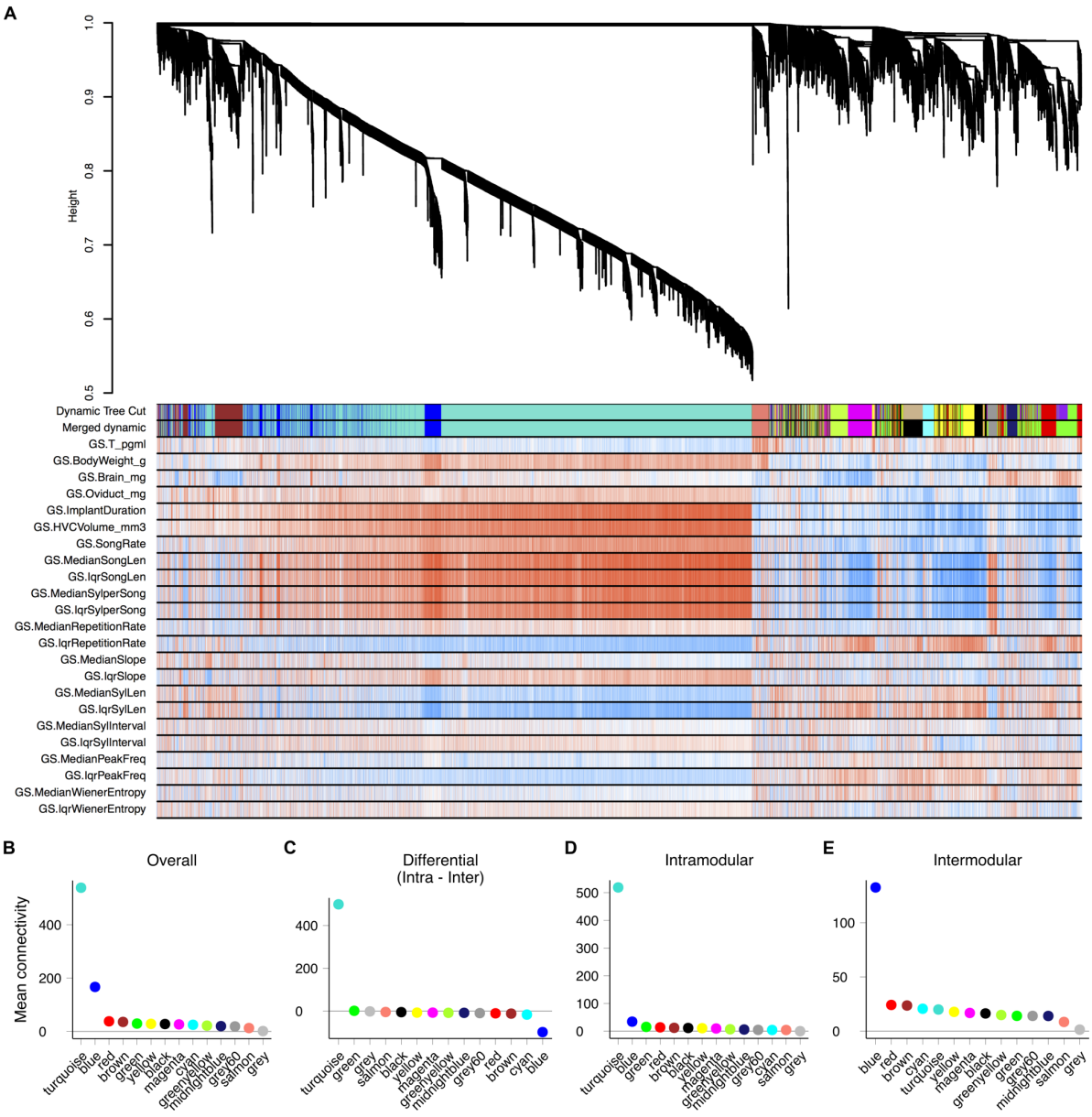

Supplementary Fig. 5. The unsupervised clustering method WGCNA classified differentially expressed genes into coexpression modules and grouped similar modules into 14 modules. A, WGCNA calculated the gene significance (GS) between the expression level of each gene and physiological traits (plasma androgen level (T), body weight, brain weight, oviduct weight, and HVC volume) and song measurements (song rate, song length, syllables per song, syllable repetition rate, syllable slope, syllable length, syllable interval, maximum frequency, entropy) by calculating the Pearson correlation matrix. Genes with positive gene significance are shown in red, while genes with negative are shown in blue. Iqr: inter-quartile range. Modules ranked by **B**, overall **C**, differential, **D**, intramodular, and **E**, intermodular connectivity. A module with high differential connectivity indicates that genes are more densely connected within the module than with the genes from other modules.

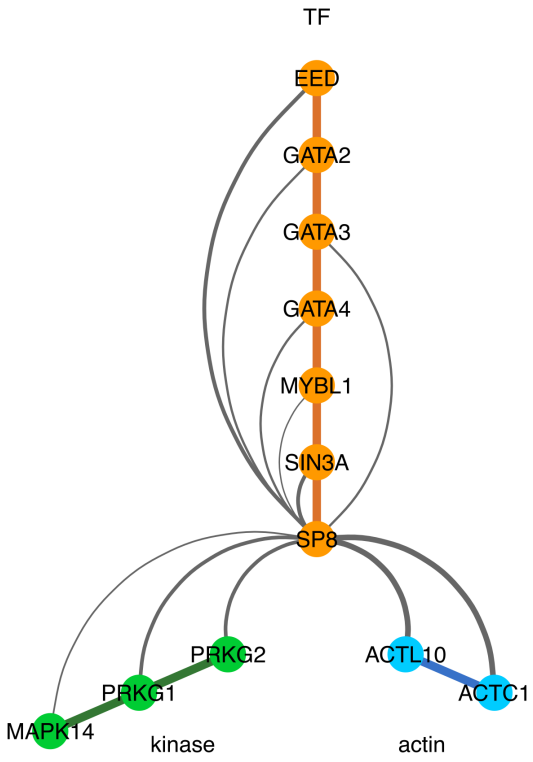

Supplementary Fig. 6. Proteins that might interact with transcription factor SP8 to regulate gene expression in the HVC. Orange circles: transcription factors (TF); green: kinases; blue: actins. The widths of the connections represent the confidence levels (with a minimum of 0.4) given by the STRING database.

1431 **Supplementary Tables and Legends.**

1432 **Supplementary Table 1. Summary table for measured song parameters (mean ± SD).**

1433 **Supplementary Table 2. Estimates of fixed and random effects of linear mixed effect models.** We
1434 present fixed (β) and random (σ2) parameters with their 95% credible intervals (CrI). A statistically
1435 meaningful effect of a fixed factor can be assumed if zero is not included within the 95% CrI, and was
1436 labeled with *.

1437 **Supplementary Table 3. The posterior probability of a mean difference between compared**
1438 **factors of linear mixed effect models.** Comparisons with statistically meaningful differences, defined
1439 by posterior probability > 0.95, were indicated with ***.**

1440 **Supplementary Table 4. List of constantly regulated genes.**

1441 **Supplementary Table 5. Over-representation of AREs and EREs in the promoter sequences of**
1442 **testosterone up-regulated genes.** Reported values are Z-scores of over-representation against the
1443 matching numbers of randomly sampled promoter sequences as the user-defined background.

1444 **Supplementary Table 6. MatInspector identified AREs and EREs in the promoter sequences of**
1445 **T1h up-regulated transcription factors.**

1446 **Supplementary Table 7. GO-term enrichment analysis of differentially expressed genes of each**
1447 **time point.**

1448 **Supplementary Table 8. Enrichment analysis of search terms using Fisher's exact test.** P-values
1449 were corrected using the "FDR" method.

1450 **Supplementary Table 9. Expression levels of genes associated with particular cell types.**

1451 **Supplementary Table 10. Connectivity and gene significance of genes assigned to the "turquoise"**
1452 **module by WGCNA.** Overall connectivity (kTotal); Intramodular connectivity (kWithin);
1453 Intermodular connectivity (kOut); Differential connectivity (kDiff). GS: gene significance.

1454 **Supplementary Table 11. Enrichment analysis of search terms of each WGCNA module.** P-
1455 values were corrected using the "FDR" method.

1456 **Supplementary Table 12. List of genes (625) contains SP8 binding sites in proximal promoter**
1457 **sequences.**

1458 **Supplementary Table 13. List of genes (169) contains SP8 and GATA binding sites in proximal**
1459 **promoter sequences.**